

# Estimation of Parameters and Design of a Path Following Controller for a Prototype AUV

*Thesis submitted in partial fulfillment  
of the requirements of the degree of*

*Bachelor of Technology (B.Tech)  
in  
Electrical Engineering*

*by*

*Satya Sundar Sahoo - 112EE0056  
Sagar Kumar - 112EE0240*

*based on the research carried out  
Under the guidance of*

*Prof. Bidyadhar Subudhi*



Department of Electrical Engineering,  
National Institute of Technology Rourkela



Department of Electrical Engineering  
**National Institute of Technology Rourkela**

---

**Prof. Bidyadhar Subudhi**  
Professor

May 10, 2016

## Supervisor's Certificate

This is to certify that the work presented in the thesis entitled *Estimation of Parameters and Design of a Path Following Controller for a Prototype AUV* submitted by *Satya Sundar Sahoo*, Roll Number 112EE0056 and *Sagar Kumar*, Roll Number 112EE240, is a record of original research carried out by them under my supervision and guidance in partial fulfillment of the requirements of the degree of *Bachelor of Technology* in *Electrical Engineering*. Neither this thesis nor any part of it has been submitted earlier for any degree or diploma to any institute or university in India or abroad.

---

Prof. Bidyadhar Subudhi

# Dedication

*This Thesis is Dedicated to,  
All our Teachers in the Department of Electrical  
Engineering, NIT Rourkela,  
to our Loving Parents and  
finally to all our Friends*

# Declaration of Originality

We, *Satya Sundar Sahoo*, Roll Number *112EE0056* and *Sagar Kumar*, Roll Number *112EE0240* hereby declare that this thesis entitled *Estimation of Parameters and Design of a Path Following Controller for a Prototype AUV* presents our original work carried out as an undergraduate student of NIT Rourkela and, to the best of our knowledge, contains no material previously published or written by another person, nor any material presented by us for the award of any degree or diploma of NIT Rourkela or any other institution. Any contribution made to this research by others, with whom we have worked at NIT Rourkela or elsewhere, is explicitly acknowledged in the thesis. Works of other authors cited in this thesis have been duly acknowledged under the sections “Reference” or “Bibliography”. We have also submitted our original research records to the scrutiny committee for evaluation of our thesis.

We are fully aware that in case of any non-compliance detected in future, the Senate of NIT Rourkela may withdraw the degree awarded to me on the basis of the present thesis.

*Satya Sundar Sahoo*  
(112EE0056)

May 10, 2016  
NIT Rourkela

*Sagar Kumar*  
(112EE0240)

# Acknowledgement

We take the opportunity to express our reverence to our supervisor Prof. Bidyadhar Subudhi for his guidance, inspiration and innovative technical discussions all during the course of this work. We find words inadequate to thank him for enabling us to complete this work in spite of all obstacles. We would also like to thank Raja Rout and Subhasish Mohaptra for their friendly support. We are also thankful to all faculty members of Electrical Engineering Department, NIT Rourkela for their support and teachings which have enabled us to move forward in life.

Special thanks to Mr. S Swain for all his support in the lab.

Its our pleasure to show our indebtedness to all of our friends at NIT for making our lives fun and joyful, which subsequently made our work easier.

# Abstract

In order to improve the performance of autonomous underwater vehicles (AUVs) deployed in different applications such as oceanographic survey, search and detection tasks in a given area necessitates the development of an appropriate path following controller which offers a precise and rapid control of the AUVs' control surfaces and propeller system. In order to design such a vehicle control system, there is a need for good approximation of the vehicles static and dynamic model. Based on a combination of theoretical and empirical data, it can provide a good starting point for vehicle control system development as well as an alternative to the typical trial-and-error methods used for controller design and tuning. As there are no standard procedure for AUV modeling, the simulation of each autonomous underwater vehicle (AUV) represents a new challenge. This thesis describes the development of a six degree of freedom, non-linear simulation model for the prototype AUV. In this model, all the forces which strongly affect the dynamic performance of an AUV such as the external forces and moments resulting from hydrostatics, hydrodynamics, lift and drag, added mass, and the control inputs of the AUV propeller and fins are all defined in terms of vehicle coefficients. Computational Fluid Dynamics along with empirical formulas have been applied to determine the hydrodynamic coefficients of the AUV. In order to model the behavior of the AUV as closely to the real-world system as possible, the equations used for determining the coefficients, as well as those describing the AUVs' motions were left in non-linear form. Simulation of the AUV motion was achieved using numerical integration techniques of the equations of motion based on the derived coefficients. From the simulation, of the AUV model, results observed led to the development of a controller for the prototype AUV. Sliding Mode Controller was chosen as the desired controller because of its definitive advantages over the PID controller, some of which are the straightforward firmware implementation, use of discrete decision rules which allows the controller to function in hybrid feedback configuration and the fact that it does not suffer from issues related with the drift in controller signal output with time, i.e. latency issues for real time applications. The developed model of the prototype AUV was decoupled into two separate parts namely Heading control and Depth control. State Space Model for each part was derived and a Sliding Mode controller was developed based on the required dynamics of each part. Simulations of the AUV model integrated with Sliding Mode Controller (SMC) was carried out to determine whether the controller was able to direct the motion of the prototype AUV along the desired path, i.e. the level of accuracy of the prototype AUV in path following task.

***Keywords: Autonomous Underwater Vehicle ; Hydrodynamic Coefficients; Sliding Mode Controller; Path Following Task***

# Contents

<b>1</b>	<b>Introduction</b>	<b>5</b>
1.1	Motivation . . . . .	5
1.2	Vehicle Model Development . . . . .	5
1.3	Modeling Assumptions . . . . .	6
<b>2</b>	<b>Prototype AUV Mechanical Parameters</b>	<b>7</b>
2.1	Body Shape . . . . .	7
2.2	Nose and Tail Shape . . . . .	9
2.3	Procedure to find Centre of Buoyancy and Inertia Tensor of the AUV	11
2.4	Calculation of Drag parameter . . . . .	11
2.4.1	Simulation Model for CFD analysis of the AUV . . . . .	11
2.4.2	Boundary Conditions and Fluid Properties . . . . .	13
2.4.3	Simulation Result . . . . .	14
2.5	AUV Mechanical Parameter . . . . .	15
<b>3</b>	<b>Determination of AUV Hydrodynamic Parameters</b>	<b>17</b>
3.1	Vectors defining AUV kinematics . . . . .	17
3.2	Hydrodynamic Damping . . . . .	17
3.2.1	Axial Drag . . . . .	18
3.2.2	Cross-flow Drag . . . . .	18
3.2.3	Rolling Drag . . . . .	19
3.3	Added Mass . . . . .	19
3.3.1	Axial Added Mass . . . . .	20
3.3.2	cross-flow Added Mass . . . . .	20
3.3.3	Rolling Added Mass . . . . .	21
3.3.4	Added Mass Cross-terms . . . . .	21
3.4	Body Lift . . . . .	22
3.4.1	Body Lift Force . . . . .	22
3.4.2	Body Lift Moment . . . . .	23
3.5	Fin Lift . . . . .	23
3.6	Propulsion Model . . . . .	25
3.6.1	Propeller Thrust . . . . .	25
3.6.2	Propeller Torque . . . . .	25
3.7	Combined Terms . . . . .	26

<b>4</b>	<b>AUV Simulation</b>	<b>27</b>
4.1	AUV Kinematics . . . . .	27
4.2	AUV Rigid-Body Dynamics . . . . .	28
4.3	Hydrostatics . . . . .	29
4.4	AUV Forces and Moments . . . . .	29
4.5	Combined Nonlinear Equations of Motion . . . . .	30
4.6	Numerical Integration of the Equations of Motion . . . . .	31
4.6.1	Runge-Kutta Method . . . . .	31
4.7	AUV Simulation Results . . . . .	32
<b>5</b>	<b>Linearised Depth Plane and Heading Plane Model of the AUV</b>	<b>34</b>
5.1	Depth Plane Model . . . . .	34
5.1.1	AUV Kinematics . . . . .	34
5.1.2	AUV Dynamics . . . . .	35
5.1.3	Linearised AUV parameter Derivation . . . . .	35
5.1.4	Linearised and Decoupled Equation of Motion of AUV in Depth Plan . . . . .	38
5.2	Heading Plane Model . . . . .	38
5.2.1	AUV Kinematics . . . . .	38
5.2.2	AUV Dynamics . . . . .	39
5.2.3	Linearised AUV parameter Derivation . . . . .	39
5.2.4	Linearised and Decoupled Equation of Motion of AUV in Heading Plane . . . . .	42
<b>6</b>	<b>Controller Design for Path Following Task</b>	<b>43</b>
6.1	Reponse of the system without any controller . . . . .	43
6.1.1	Depth Plane System . . . . .	43
6.1.2	Heading Plane System . . . . .	45
6.2	Sliding Mode Controller (SMC) . . . . .	46
6.3	Control Law derivation . . . . .	47
6.3.1	Depth Plane Control . . . . .	47
6.3.2	Heading Plane Control . . . . .	49
<b>7</b>	<b>Conclusion</b>	<b>51</b>
7.1	Scope for Future Research . . . . .	52
	<b>Appendix</b>	<b>53</b>
	Appendix A - AUV Parameters . . . . .	53
	Appendix B - Matlab Codes . . . . .	55
	Matlab Code for AUV Simulation . . . . .	55
	Matlab Code to Calculate Hydrodynamic Coefficients . . . . .	59
	Depth Plane Controller Design . . . . .	60
	Heading Plane Controller Design . . . . .	62



# List of Figures

2.1	Prototype AUV . . . . .	7
2.2	Body <i>Shape</i> <sup>[22]</sup> . . . . .	8
2.3	2D Drawing of the Actual AUV . . . . .	8
2.4	Radius of Nose vs Length . . . . .	9
2.5	Nose section . . . . .	9
2.6	Radius of Tail section vs. Length . . . . .	10
2.7	Tail Section . . . . .	10
2.8	Volume and Mass analysis tool . . . . .	11
2.9	Meshed AUV Structure in ANSYS . . . . .	13
2.10	$C_{df}$ vs Length of AUV . . . . .	14
2.11	$C_{dp}$ vs Length of AUV . . . . .	14
2.12	2D figure of Prototype AUV . . . . .	15
4.1	AUV Motion in XYZ plane for stern angle=0° and rudder angle=0°	32
4.2	AUV Motion in XYZ plane for stern angle=30° and rudder angle=0°	33
4.3	AUV Motion in XYZ plane for stern angle=0° and rudder angle=30°	33
5.1	Velocity squared vs. Velocity . . . . .	36
5.2	Velocity squared vs. Velocity . . . . .	40
6.1	Root Locus Plot of the Depth Plane System . . . . .	44
6.2	Response of the Depth Plane system (Depth vs. time) . . . . .	44
6.3	Root Locus Plot of the Heading Plane System . . . . .	45
6.4	Response of the Heading Plane system (Heading ( $\psi$ ) vs. time) . . .	45
6.5	System Response to Step Input Trajectory (Depth vs Time) . . . .	48
6.6	System Response to ramp input trajectory (Depth vs. Time) . . . .	48
6.7	System Response to Step Input Trajectory (Heading( $\psi$ ) vs Time . .	49
6.8	System Response to ramp input trajectory (Heading( $\psi$ ) vs. Time) .	50

# List of Tables

2.1	Boundary Conditions for Simulation . . . . .	13
2.2	Fluid Properties . . . . .	13
2.3	AUV Hull Parameters . . . . .	15
2.4	Hull coordinates for limit of integration . . . . .	15
2.5	Centre of Buoyancy wrt origin at AUV nose . . . . .	16
2.6	Centre of Gravity wrt Origin at CB . . . . .	16
2.7	AUV Fin parameters . . . . .	16
2.8	Inertia Values of AUV along different axis . . . . .	16
3.1	Values of drag coefficients . . . . .	19
3.2	Values of added mass . . . . .	22
3.3	Values of added mass cross-terms . . . . .	23
3.4	Body Lift Coefficients . . . . .	24
3.5	Fin lift coefficients . . . . .	24
3.6	Propeller parameter . . . . .	25
5.1	Value of Linearised Coefficients . . . . .	37
5.2	Value of Linearised Coefficients . . . . .	41

# Chapter 1

## Introduction

### 1.1 Motivation

In the last millennium, there has been an ever growing interest in autonomous vehicles for a variety of purposes which pose a hazard for the human life. These include deep sea surveys, space explorations and even in fighting wars. See for example, [36,37,38] and references therein for a survey of existing prototype AUVs and their proposed applications. But this area has really exploded in last 2 decades with the advent of miniaturized electronic sensors, technological know-how, development of high bandwidth communication systems and low power consuming propulsion systems. Already, we have seen a variety of semi-autonomous vehicles in production like, the Predator Unmanned Aerial Vehicle, NASA's Mars Rover etc. But these vehicles still need an umbilical cord attached with their human controllers for constant supervision and proper completion of their mission objectives. Therefore, much work still remains in the area of accurate guidance and control systems which will lead to these vehicles becoming truly autonomous.

Motivated by these requirements, this thesis tackles the problem of developing low cost methodologies for the development of the controller and guidance systems for AUVs. A dynamic vehicle model based on a combination of theoretical formulas and empirical data can provide an efficient starting point for the development of vehicle control system, and offer an alternative to the typical trial-and-error method of vehicle control system field tuning, which leads to escalation of cost and development time. As there are no set standards for vehicle modeling, simulation of each and every vehicle system represents a new challenge.

### 1.2 Vehicle Model Development

This thesis describes in detail the method used to model the six degree of freedom prototype AUV. In general, the external forces and torques which are generated due to the hydrostatics, hydrodynamic lift and drag, added mass, control surface inputs and the thrusters have been well defined in terms of vehicle parameter.

Derivation of these coefficients has been discussed in this thesis using empirical formula and computational fluid dynamics. The derived coefficients were used to model the prototype AUV in MATLAB using the kinematics and vehicle rigid

body dynamics equations. All the above equations were left in non linear form for better approximation of the system.

In the development of the controller, AUV motion was linearised and decoupled into two different parts Heading Plane and Depth Plane. This enabled us to build separately controller for each part based on required dynamics of heading and depth plane motion.

### 1.3 Modeling Assumptions

Some of the assumptions taken into account while developing the model of the AUV were,

- Vehicle was assumed to be present in deep sea conditions, i.e. no surface disturbances like waves.
- Vehicle is not affected by underwater current.
- Vehicle body is rigid and it's mass remains constant under any operating condition.
- The control surfaces do not stall under any angle of attack of the water, while they are within their operating range.
- We have assumed a constant speed thruster operation, i.e the thruster provides a constant thrust to the vehicle.

# Chapter 2

## Prototype AUV Mechanical Parameters

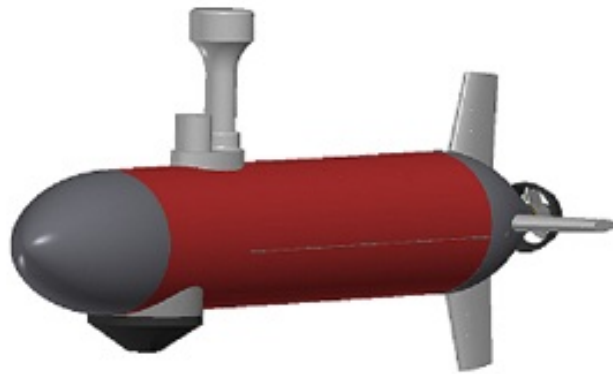


Figure 2.1: Prototype AUV

The above figure shows the representative CAD model of the prototype AUV built in the Department of Electrical Engineering, National Institute of Technology, Rourkela. Torpedo shape with 4 fins and one thruster configuration was chosen, for the simple fact that the torpedo shape offers a symmetrical design with low drag and greater overall stability. The above given shape of nose and tail were created using the standards defined by Myring [4].

### 2.1 Body Shape

The above figure shows the general body shape of the torpedo type AUV as laid out by Myring. In the above figure, 'a' is the length of the nose, 'b' length of the cylindrical body, 'c' length of the tail section, 'L' total length of the AUV, 'r' radius of the AUV at each point, 'd' maximum diameter of the body and '2θ' the included angle at the tip.

Nose shape is given by the modified elliptical shape radius distribution,

$$r = \frac{1}{2}d \left\{ 1 - \left( \frac{x-a}{a} \right)^2 \right\}^{\frac{1}{n}} \quad (2.1)$$

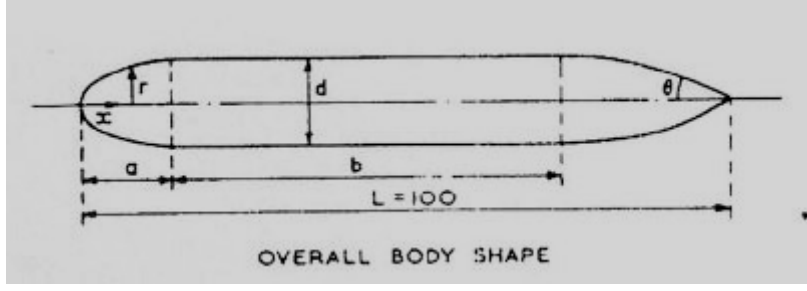


Figure 2.2: Body *Shape*<sup>[22]</sup>

Tail shape is given by the cubic relationship,

$$r = \frac{d}{2} - \left\{ \frac{3d}{2(L - a - b)^2} - \frac{\tan \theta}{(L - a - b)} \right\} \{x - a - b\}^2 + \left\{ \frac{d}{(L - a - b)^3} - \frac{\tan \theta}{(L - a - b)^2} \right\} \{x - a - b\}^3 \quad (2.2)$$

The above two equations were used to determine the shape of the AUV. However, because the AUV was handmade there were some deviations from the ideal nose and tail shape. In order to find the actual nose and tail shape equations following procedure was adopted,

- Photographs of the AUV were taken from various angle.
- Photographs were imported into the solidworks software and a 2D drawing of the actual AUV was made.
- From the 2D drawing radius of the tail and nose were sampled at various intervals.

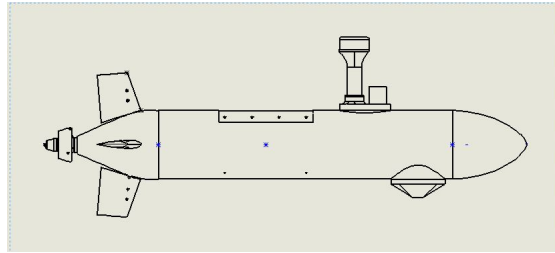


Figure 2.3: 2D Drawing of the Actual AUV

Thus, from the above 2D drawing actual radius of nose and tail at various points were measured and equations formed.

## 2.2 Nose and Tail Shape

Radius of Nose sampled from the actual 2D drawing of the AUV is given as follows. The modified equation of the nose obtained after curve fitting,

$$R(x) = 2.98 \times 10^{-5} x^5 - 0.0015 x^4 + 0.0279 x^3 - 0.2692 x^2 + 1.7476 x + 0.27283 \quad (2.3)$$

x (cm)	R(x) (cm)	x (cm)	R(x) (cm)
0	0	7.38	6.03
0.08	0.42	7.88	6.22
0.36	1.03	8.47	6.43
0.7	1.52	9.19	6.67
1.14	2.05	9.88	6.87
1.65	2.58	10.4	7.01
2.17	3.04	10.81	7.11
2.65	3.42	11.38	7.24
2.98	3.67	11.91	7.36
3.28	3.88	12.56	7.48
3.6	4.09	13.05	7.56
4.03	4.37	13.62	7.64
4.34	4.56	14.17	7.72
4.78	4.8	14.74	7.78
5.31	5.09	15.28	7.83
5.7	5.29	15.71	7.86
6.28	5.56	16.34	7.9
6.75	5.77	17.26	7.95

Figure 2.4: Radius of Nose vs Length

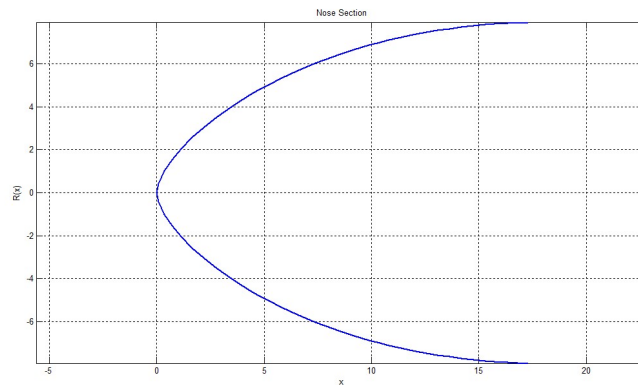


Figure 2.5: Nose section

Radius of Tail section sampled from the actual 2D drawing of the AUV is given as follows. The modified equation of the nose obtained after curve fitting,

$$T(x) = 0.0019x^3 - 0.0477x^2 + 0.1236x + 7.95 \quad (2.4)$$

x	R(x)	x	R(x)
85.86	7.95	97.63	5.17
86.4	8.01	97.9	5.04
86.94	8.04	98.14	4.94
87.48	8.04	98.37	4.84
87.89	8.02	98.63	4.72
88.31	8	98.86	4.62
88.91	7.94	99.11	4.51
89.72	7.82	99.38	4.38
90.23	7.73	99.58	4.29
90.55	7.66	99.78	4.2
91.11	7.53	99.98	4.09
91.57	7.41	100.23	3.99
92.17	7.24	100.64	3.8
92.73	7.07	100.97	3.65
93.34	6.88	101.32	3.49
93.78	6.72	101.61	3.36
94.19	6.58	101.94	3.22
94.56	6.44	102.29	3.05
95.02	6.26	102.45	2.99
95.4	6.12	102.76	2.86
95.96	5.89	102.99	2.76
96.48	5.67	103.22	2.66
96.89	5.49	103.49	2.54
97.18	5.37	104.08	2.3
97.44	5.25	104.77	2.02

Figure 2.6: Radius of Tail section vs. Length

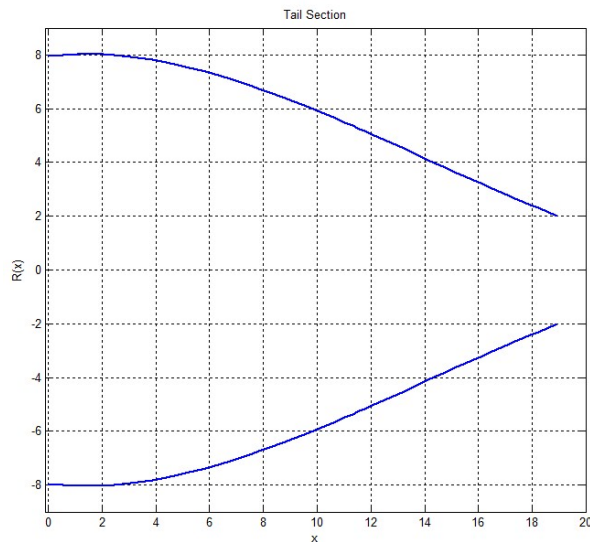


Figure 2.7: Tail Section



## 2.3 Procedure to find Centre of Buoyancy and Inertia Tensor of the AUV

It was imperative to find the centre of buoyancy and inertia tensor of the AUV, in order to proceed with the calculation of coefficients. The procedure adopted for this is as follows,

- The 2D drawing created before was converted to 3D, and the entire volume was simulated to be filled with water in solidworks.
- The mass and volume analysis tool of the solidworks software was then used to find the centre of buoyancy and inertia tensor of the AUV.

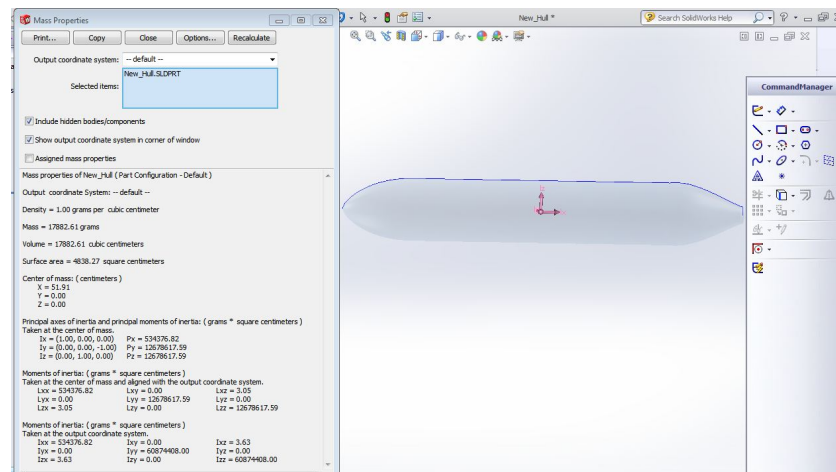


Figure 2.8: Volume and Mass analysis tool

## 2.4 Calculation of Drag parameter

Drag is the resistance offered by a fluid to the relative motion of a body in that fluid. Drag parameter is a dimensionless quantity which is used to quantify the drag experienced by the body. In order to calculate the hydrodynamic coefficients of the AUV which affect the drag force, we need to calculate the drag parameter of the AUV. To do this, Computational Fluid Dynamics was carried out in *ANSYS Software*. General Procedure used was,

- 3D CAD model of the AUV was imported into the software.
- Boundary layer was defined.
- Simulation model was setup.

### 2.4.1 Simulation Model for CFD analysis of the AUV

To investigate the single phase flow of seawater around the hull of the AUV, a permanent incompressible and isothermal turbulent flow was considered. Following equations were used to model the flow,

1. Mass Conservation Equation

$$\frac{\partial \delta}{\partial t} + \nabla \cdot (\rho U) = 0 \quad (2.5)$$

$U$  = velocity,  $\rho$  = Density of water

2. Momentum Conservation System

$$\frac{\partial U}{\partial t} + \nabla(\rho U x U) - \nabla(\mu \nabla U) = -\nabla P' + \nabla(\mu \nabla U^T) + \rho g \quad (2.6)$$

$P'$  = Corrected Pressure,  $g = 9.81 m/s^2$ ,  $\mu$  = viscosity of water

Turbulence in general is caused by surface roughness and sea conditions. In the model used for CFD analysis Shear Stress Turbulence based on  $k-\omega$  model was used.

3. Turbulent Kinetic Energy,

$$\frac{\partial \rho k}{\partial t} + \nabla(\rho U k) = \nabla \cdot \left[ \left( \mu + \frac{\mu}{C_{k1}} \right) \nabla k \right] + P_k - C_{k2} \rho k \omega \quad (2.7)$$

$$C_{k1} = 2, C_{k2} = 0.009$$

4. Turbulence Energy Equation

$$\frac{\partial \rho \omega}{\partial t} + \nabla(\rho U \omega) = \nabla \cdot \left[ \left( \mu + \frac{\mu_t}{C_{\omega 1}} \right) \nabla \omega \right] + \frac{\omega}{k} (C_{\omega 2} P_k - C_{\omega 3} \rho \omega k) \quad (2.8)$$

$$C_{\omega 1} = 2, C_{\omega 2} = 0.556, C_{\omega 3} = 0.075$$

$$\mu_t = \frac{\rho k}{\omega}, k = \text{kinetic energy}$$

Viscosity diminishes the velocity of a fluid past a surface and thus decreases the momentum of the fluid. Since, the fluid flow is governed by pressure distribution around the hull of the AUV, we must consider both the retarding action of the viscosity and the imposed pressure distribution.

This is done by calculating the drag parameter,

$$C_d = C_{df} + C_{dp} = \frac{F_{df}}{\frac{1}{2} \rho U^2 A_f} + \frac{F_{dp}}{\frac{1}{2} \rho U^2 A_f} \quad (2.9)$$

$F_{df}$  = Frictional Drag Force,  $F_{dp}$  = Pressure drag force,  $A_f$  = AUV Frontal Area

## 2.4.2 Boundary Conditions and Fluid Properties

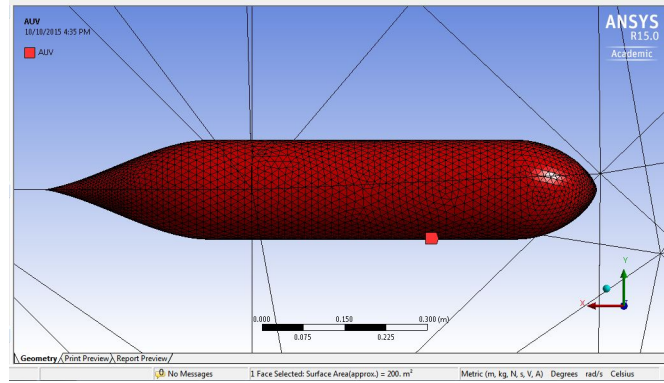


Figure 2.9: Meshed AUV Structure in ANSYS

Boundary	Parameter	Value
Inlet	Velocity	1.5 m/s
Wall	Pressure	10.2 MPa
AUV Hull	Velocity	0 m/s
Outlet	Pressure	10.2 MPa

Table 2.1: Boundary Conditions for Simulation

Type of Water	Salt Water
Density	1030 $\text{Kg}/\text{m}^3$
Viscosity	1.19 mPa-s

Table 2.2: Fluid Properties

### 2.4.3 Simulation Result

The following results were obtained from the CFD analysis of the AUV Model,

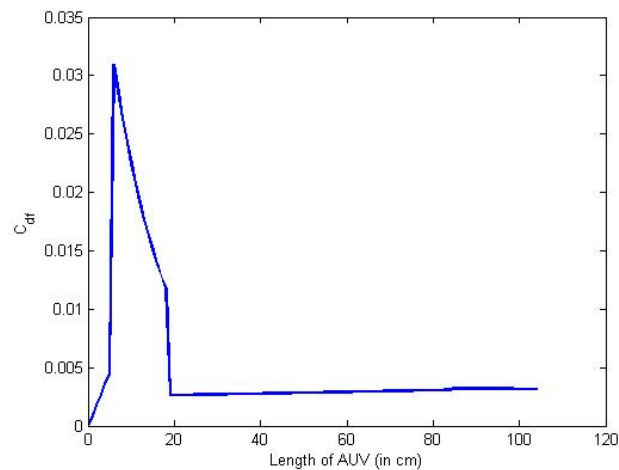


Figure 2.10:  $C_{df}$  vs Length of AUV

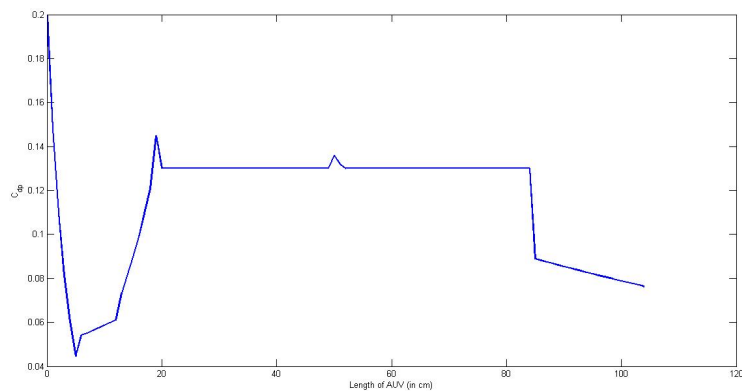


Figure 2.11:  $C_{dp}$  vs Length of AUV

From the above two graphs it is observed that the value of the drag coefficients varies along the surface of the AUV body, this can be attributed to the fact that the shape of AUV can be divided into three different parts, the nose, body and the tail section.

The Drag due to pressure is less near the nose section because the water has to traverse a longer distance as compared to the main hull. So, the velocity of water is more this also leads to higher drag because of liquid friction. But on the main body value of both the drags settles down to a almost constant value.

Thus, the Drag parameter of the AUV in the salt water is,

$$C_d = 0.13 + 0.003 = 0.133$$

## 2.5 AUV Mechanical Parameter

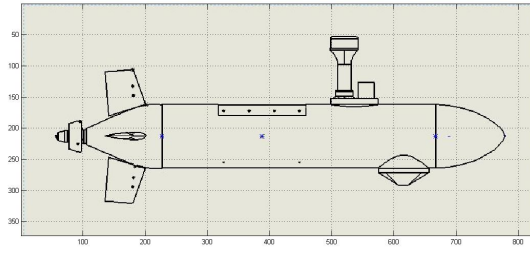


Figure 2.12: 2D figure of Prototype AUV

Parameter	Value	Units	Description
$\rho$	1030	$kg/m^3$	Seawater Density
a	17.26	cm	Length of Nose Section
b	68.60	cm	Length of Midsection
c	18.91	cm	Length of Tail Section
L	104.77	cm	Total length of AUV
d	15.9	cm	Maximum diameter of the Hull
$A_f$	198.806	$cm^2$	Hull frontal Area
V	0.017882	$m^3$	Volume of AUV
W	174.68	N	Measured AUV weight
B	196.2	N	Measured AUV Buoyancy
$C_d$	0.133	n/a	AUV Axial drag parameter
$C_{dc}$	1.1	n/a	Cylinder cross-flow drag parameter
$C_{yd\beta}$	1.1326	n/a	Hoerner's Lift parameter
$C_{dfin}$	0.6072	n/a	Fin cross-flow Drag parameter
$x_{cp}$	-0.1619	m	Centre of Pressure

Table 2.3: AUV Hull Parameters

Parameter	Value	Units	Description
$x_t$	-0.5286	m	Aft end of tail section
$x_{t2}$	-0.3395	m	Forward end of tail section
$x_f$	-0.4747	m	Aft end of Fin section
$x_{f2}$	-0.3920	m	Forward end of Fin section
$x_b$	0.3465	m	Aft end of bow/nose section
$x_{b2}$	0.5191	m	Forward end of nose/bow section

Table 2.4: Hull coordinates for limit of integration

Parameter	Value	Units
$x_{cb}$	-0.5191	m
$y_{cb}$	0	m
$z_{cb}$	0	m

Table 2.5: Centre of Buoyancy wrt origin at AUV nose

Parameter	Value	Units
$x_{cg}$	0	m
$y_{cg}$	0	m
$z_{cg}$	0.02	m

Table 2.6: Centre of Gravity wrt Origin at CB

Parameter	Value	Units	Description
Fin Profile	NACA0020	n/a	n/a
$S_{fin}$	0.008645	$m^2$	Planform Area
$b_{fin}$	0.0874	m	Span
$a_{fin}$	0.1673	m	Height oh Fin above AUV body Centre Line
t	0.7246	n/a	Fin Taper Ratio
$AR_e$	1.7665	n/a	Aspect Ratio
$C_{L\alpha}$	2.8	n/a	fin Lift Slope
$x_{finpost}$	-40.78	m	Moment arm of fin wrt CB

Table 2.7: AUV Fin parameters

Inertia	Value	Unit
$I_{xx}$	0.0534	$kg - m^2$
$I_{yy}$	1.267	$kg - m^2$
$I_{zz}$	1.267	$kg - m^2$

Table 2.8: Inertia Values of AUV along different axis

# Chapter 3

## Determination of AUV Hydrodynamic Parameters

In this chapter, we will derive the values of drag , added mass, body lift, fin lift and propeller coefficients, which define the forces and moments acting on the AUV. For calculation of each of the coefficients, the required AUV parameter and the surrounding fluid parameter is included in the chapter.

### 3.1 Vectors defining AUV kinematics

The movement of the body-fixed frame of reference is depicted in respect to an inertial or earth-fixed reference frame. The general movement of the AUV in six degrees of freedom can be depicted by the following vectors:

$$\begin{aligned}\eta_1 &= [x \ y \ z]^T \\ \eta_2 &= [\phi \ \theta \ \psi]^T \\ \nu_1 &= [u \ v \ w]^T \\ \nu_2 &= [p \ q \ r]^T \\ \tau_1 &= [X \ Y \ Z]^T \\ \tau_2 &= [K \ M \ N]^T\end{aligned}$$

where,  $\eta$  describes the position and orientation vector of the AUV with respect to the earth fixed reference frame,  $\nu$  the translational and rotational velocities of the AUV with respect to the body-fixed reference frame, and  $\tau$  the total forces and moments acting on the AUV with respect to the body-fixed reference frame.

### 3.2 Hydrodynamic Damping

It is well understood that the damping of an underwater vehicle moving at a high speed in six degrees of freedom is coupled and profoundly non-linear. For simplification of the modeling of the AUV, following assumption were made:

- The linear and angular coupled terms are neglected.
- AUV is symmetric about XY-plane and XZ-plane.
- Damping terms greater than second order are neglected.

The main cause of hydrodynamic damping are frictions because of the boundary layers, which are partially laminar and partially turbulent. Non-dimensional analysis helps in predicting the flow type across the AUV. Reynolds number represents the ratio of inertial to viscous forces, and is given by the equation:

$$Re = \frac{Ul}{\nu} \quad (3.1)$$

where,

$U$  is speed of the AUV

$l$  is length of the AUV

$\nu$  is the fluid kinematic viscosity.

The value of the Reynold's number for our AUV is  $1.412 \times 10^6$ .

### 3.2.1 Axial Drag

The non-linear axial drag parameter can be obtained from the following equation:

$$X_{u|u} = -\frac{1}{2}\rho c_d A_f \quad (3.2)$$

where,

$A_f$  is AUV frontal area

$c_d$  is the axial drag parameter of the AUV

$\rho$  is the density of the surrounding fluid.

### 3.2.2 Cross-flow Drag

Summation of the hull cross-flow drag and the fin cross-flow drag leads to the total AUV cross-flow drag. The procedure for calculation of hull drag is similar to that of Strip Theory. The total hull drag is considered to be the summations of the drags on the cross-sections of the two-dimensional cylindrical AUV.

The non-linear cross-flow drag coefficients are given by the following equations:

$$\begin{aligned} Y_{v|v} = Z_{w|w} &= -\frac{1}{2}\rho c_{dc} \int_{x_t}^{x_{b2}} 2R(x)dx - 2 \cdot \left(\frac{1}{2}\rho S_{fin} c_{df}\right) \\ M_{w|w} = -N_{v|v} &= \frac{1}{2}\rho c_{dc} \int_{x_t}^{x_{b2}} 2xR(x)dx - 2x_{fin} \cdot \left(\frac{1}{2}\rho S_{fin} c_{df}\right) \\ Y_{r|r} = -Z_{q|q} &= -\frac{1}{2}\rho c_{dc} \int_{x_t}^{x_{b2}} 2x|x|R(x)dx - 2x_{fin}|x_{fin}| \cdot \left(\frac{1}{2}\rho S_{fin} c_{df}\right) \\ M_{q|q} = N_{r|r} &= -\frac{1}{2}\rho c_{dc} \int_{x_t}^{x_{b2}} 2Rx^3(x)dx - 2x_{fin}^3 \cdot \left(\frac{1}{2}\rho S_{fin} c_{df}\right) \end{aligned} \quad (3.3)$$

where,

$c_{dc}$  is the drag parameter of the cylinder

$c_{df}$  is the drag parameter of the control fins



$R(x)$  is the hull radius as a function of axial position,  $x$   
 $\rho$  is the density of the surrounding fluid.  
 $S_{fin}$  is control fin platform area.

Cross-flow drag parameter of a cylinder,  $c_{dc}$  is estimated to be 1.1.  
The cross-flow drag parameter of the control fins,  $c_{df}$  can be found out using the below formula:

$$c_{df} = 0.1 + 0.7t \quad (3.4)$$

where,  
 $t$  is the fin taper ratio.

### 3.2.3 Rolling Drag

Rolling resistance of the AUV is approximated by assuming that the principle component comes from the cross-flow drag of the fins.

The rolling drag parameter is given by:

$$K_{p|p|} = Y_{v|v|} r_{mean}^3 \quad (3.5)$$

where,  
 $Y_{v|v|}$  is the fin component of the AUV cross-flow drag parameter  
 $r_{mean}$  is the mean fin height above the AUV center line.

The values of drag coefficients are summarised in the table below:

Parameter	Value	Units	Description
$X_{u u }$	-1.36	$kg/m$	Axial Drag
$Y_{v v }$	-90.9473	$kg/m$	Cross-flow Drag
$Y_{r r }$	0.9930	$kg.m/rad^2$	Cross-flow Drag
$Z_{w w }$	-90.9473	$kg/m$	Cross-flow Drag
$Z_{q q }$	-0.9930	$kg.m/rad^2$	Cross-flow Drag
$M_{w w }$	2.0298	$kg$	Cross-flow Drag
$M_{q q }$	0.4173	$kg.m^2/rad^2$	Cross-flow Drag
$N_{v v }$	-2.0298	$kg$	Cross-flow Drag
$N_{r r }$	0.4173	$kg.m^2/rad^2$	Cross-flow Drag
$K_{p p }$	-0.085	$kg.m^2/rad^2$	Rolling Drag

Table 3.1: Values of drag coefficients

## 3.3 Added Mass

Added mass is expressed as a measure of the mass of the moving water when the AUV accelerates.

Due to the symmetry of the AUV about XY-plane and XZ-plane, the AUV added

mass matrix reduces to:

$$\begin{bmatrix} m_{11} & 0 & 0 & 0 & 0 & 0 \\ 0 & m_{22} & 0 & 0 & 0 & m_{26} \\ 0 & 0 & m_{33} & 0 & m_{35} & 0 \\ 0 & 0 & 0 & m_{44} & 0 & 0 \\ 0 & 0 & m_{53} & 0 & m_{55} & 0 \\ 0 & m_{62} & 0 & 0 & 0 & m_{66} \end{bmatrix} \quad (3.6)$$

Which can also be written as:

$$\begin{bmatrix} X_{\dot{u}} & 0 & 0 & 0 & 0 & 0 \\ 0 & Y_{\dot{v}} & 0 & 0 & 0 & N_{\dot{v}} \\ 0 & 0 & Z_{\dot{w}} & 0 & M_{\dot{w}} & 0 \\ 0 & 0 & 0 & K_{\dot{p}} & 0 & 0 \\ 0 & 0 & Z_{\dot{q}} & 0 & M_{\dot{q}} & 0 \\ 0 & Y_{\dot{r}} & 0 & 0 & 0 & N_{\dot{r}} \end{bmatrix} \quad (3.7)$$

### 3.3.1 Axial Added Mass

For estimation of axial added mass, AUV hull shape is approximated by an ellipsoid whose major axis is half of the AUV length,  $l$  and the minor axis half of the AUV diameter,  $d$ .

The axial added mass is given by the below formula:

$$X_{\dot{u}} = -m_{11} = -\frac{4\alpha\rho\pi}{3}\left(\frac{l}{2}\right)\left(\frac{d}{2}\right)^2 = -\frac{4\beta\rho\pi}{3}\left(\frac{d}{2}\right)^3 \quad (3.8)$$

where,

$\rho$  is the density of the surrounding fluid

$\alpha$  and  $\beta$  are empirical parameters which are determined by the ratio of the AUV length to the diameter.

For our AUV the values of  $\alpha$  and  $\beta$  are 0.03585 and 0.251 respectively.

### 3.3.2 cross-flow Added Mass

Strip theory is used to calculate the AUV added mass for both cylindrical and cruciform hull cross sections.

The added mass of a single cylinder unit per unit length is given by:

$$m_a(x) = \pi\rho R(x)^2 \quad (3.9)$$

where,

$\rho$  is the density of the surrounding fluid

$R(x)$  is the hull radius as a function of axial position,  $x$ .

The added mass of a circle with fins is given by:

$$m_{af}(x) = \pi\rho(a_{fin}^2 - R(x)^2) + \frac{R(x)^4}{a_{fin}^2} \quad (3.10)$$

where,

$a_{fin}$  is the maximum height of the AUV fins above the center line.

The non-linear cross-flow added mass coefficients are given by the following equations:

$$\begin{aligned}
Y_{\dot{v}} = -m_{22} &= - \int_{x_t}^{x_f} m_a(x) dx - \int_{x_f}^{x_{f2}} m_{af}(x) dx - \int_{x_{f2}}^{x_{b2}} m_a(x) dx \\
M_{\dot{w}} = -m_{53} &= - \int_{x_t}^{x_f} x m_a(x) dx - \int_{x_f}^{x_{f2}} x m_{af}(x) dx - \int_{x_{f2}}^{x_{b2}} x m_a(x) dx \\
M_{\dot{q}} = -m_{55} &= - \int_{x_t}^{x_f} x^2 m_a(x) dx - \int_{x_f}^{x_{f2}} x^2 m_{af}(x) dx - \int_{x_{f2}}^{x_{b2}} x^2 m_a(x) dx
\end{aligned} \tag{3.11}$$

$$\begin{aligned}
Z_{\dot{w}} = -m_{33} &= -m_{22} = Y_{\dot{v}} \\
N_{\dot{v}} = -m_{62} &= -m_{53} = M_{\dot{w}} \\
Y_{\dot{r}} = -m_{26} &= -m_{62} = N_{\dot{v}} \\
Z_{\dot{q}} = -m_{35} &= -m_{53} = M_{\dot{w}} \\
N_{\dot{r}} = -m_{66} &= -m_{55} = M_{\dot{q}}
\end{aligned} \tag{3.12}$$

### 3.3.3 Rolling Added Mass

While determining the rolling added mass, it is assumed that the smoother sections of the vehicle hull do not produce added mass in roll. The hull section having the vehicle control fins is only considered while calculating the rolling added mass. The parameter of the rolling added mass is given by the following empirical formula:

$$K_{\dot{p}} = - \int_{x_{fin}}^{x_{fin}^2} \frac{2}{\pi} \rho a^4 dx \tag{3.13}$$

where,

$a$  is the maximum height of the AUV fins above the center line.

### 3.3.4 Added Mass Cross-terms

$$\begin{aligned}
X_{wq} &= Z_{\dot{w}} \\
X_{qq} &= Z_{\dot{q}} \\
X_{vr} &= -Y_{\dot{v}} \\
X_{rr} &= -Y_{\dot{r}}
\end{aligned} \tag{3.14}$$

$$\begin{aligned}
Y_{ur} &= X_{\dot{u}} \\
Y_{wp} &= -Z_{\dot{w}} \\
Y_{pq} &= -Z_{\dot{q}}
\end{aligned} \tag{3.15}$$

$$\begin{aligned}
Z_{uq} &= -X_{\dot{u}} \\
Z_{vp} &= Y_{\dot{v}} \\
Z_{rp} &= Y_{\dot{r}}
\end{aligned} \tag{3.16}$$

$$\begin{aligned}
M_{uva} &= -(Z_{\dot{v}} - X_{\dot{u}}) \\
M_{vp} &= -Y_{\dot{r}} \\
M_{rp} &= (K_{\dot{p}} - N_{\dot{r}}) \\
M_{uq} &= -Z_{\dot{q}}
\end{aligned} \tag{3.17}$$

$$\begin{aligned}
N_{uva} &= -(X_{\dot{u}} - Y_{\dot{v}}) \\
N_{wp} &= Z_{\dot{q}} \\
N_{pq} &= -(K_{\dot{p}} - M_{\dot{q}}) \\
N_{ur} &= Y_{\dot{r}}
\end{aligned} \tag{3.18}$$

Parameter	Value	Units	Description
$X_{\dot{u}}$	-0.57858	$kg$	Axial Added Mass
$Y_{\dot{v}}$	-24.0189	$kg$	Cross-flow Added Mass
$Y_{\dot{r}}$	-2.2586	$kg.m/rad$	Cross-flow Added Mass
$Z_{\dot{v}}$	-24.0189	$kg$	Cross-flow Added Mass
$Z_{\dot{q}}$	2.2586	$kg.m/rad$	Cross-flow Added Mass
$M_{\dot{v}}$	2.2586	$kg.m$	Cross-flow Added Mass
$M_{\dot{q}}$	-2.3441	$kg.m^2/rad$	Cross-flow Added Mass
$N_{\dot{v}}$	-2.2586	$kg.m$	Cross-flow Added Mass
$N_{\dot{r}}$	-2.3441	$kg.m^2/rad$	Cross-flow Added Mass
$K_{\dot{p}}$	-0.0416	$kg.m^2/rad$	Rolling Added Mass

Table 3.2: Values of added mass

## 3.4 Body Lift

Vehicle body lift is because of the vehicle movement through the water at an angle of attack, which causes separation in flow and a subsequent decrease in pressure along the aft and the upper part of the vehicle hull. The decrease in pressure can be modeled as a point force which is applied at the center of pressure.

### 3.4.1 Body Lift Force

The empirical formula for body lift parameter is given as:

$$Y_{wvl} = Z_{wvl} = -\frac{1}{2}\rho d^2 c_{yd\beta} \tag{3.19}$$

where,

$$c_{yd\beta} = c_{yd\beta}^o \left(\frac{180}{\pi}\right) \tag{3.20}$$

and,

$$c_{yd\beta}^o = \left(\frac{l}{d}\right) c_{y\beta}^o \tag{3.21}$$

Parameter	Value	Units	Description
$X_{wq}$	-24.0189	$kg/rad$	Added mass cross-term
$X_{qq}$	2.2586	$kg.m/rad$	Added mass cross-term
$X_{vr }$	24.0189	$kg/rad$	Added mass cross-term
$X_{rr}$	2.2586	$kg.m/rad$	Added mass cross-term
$Y_{ura}$	-0.57858	$kg/rad$	Added mass cross-term
$Y_{wp}$	24.0189	$kg/rad$	Added mass cross-term
$Y_{pq}$	-2.2586	$kg.m/rad$	Added mass cross-term
$Z_{uqa}$	0.57858	$kg/rad$	Added mass cross-term
$Z_{vp}$	-24.0189	$kg/rad$	Added mass cross-term
$Z_{rp}$	-2.2586	$kg/rad$	Added mass cross-term
$M_{uqa}$	-2.2586	$kg.m/rad$	Added mass cross-term
$M_{uva}$	23.44	$kg$	Added mass cross-term
$M_{vp }$	2.3025	$kg.m/rad$	Added mass cross-term
$M_{rp}$	2.3025	$kg.m^2/rad^2$	Added mass cross-term
$N_{uva}$	-23.44	$kg$	Added mass cross-term
$N_{ura}$	-2.2586	$kg.m/rad$	Added mass cross-term
$N_{wp}$	2.2586	$kg.m/rad$	Added mass cross-term
$N_{pq}$	-2.3025	$kg.m^2/rad^2$	Added mass cross-term

Table 3.3: Values of added mass cross-terms

where

$l$  is the length of the AUV

$d$  is the diameter of the AUV.

For our AUV,  $c_{y\beta}^o=0.003$ .

### 3.4.2 Body Lift Moment

For a body revolving at an angle of attack, the viscous force is centered at a point between 60-70% of the total body length from the nose.

The empirical formula for body lift moment is given as:

$$M_{uwl} = -N_{uwl} = -\frac{1}{2}\rho d^2 c_{y\beta} x_{cp} \quad (3.22)$$

where,

$$x_{cp} = -0.65l - x_{zero} \quad (3.23)$$

## 3.5 Fin Lift

The position of the AUV is controlled by the control fins whose movement depends on the stern angle and rudder angle inputs.

The set of equations which gives the fin lift coefficients are given below:

Parameter	Value	Units	Description
$Y_{uwl}$	-14.75	$kg/m$	Body Lift Force
$Z_{uwl}$	-14.75	$kg/m$	Body Lift Force
$M_{uwl}$	-2.62	$kg$	Body Lift Moment
$N_{uwl}$	2.62	$kg$	Body Lift Moment

Table 3.4: Body Lift Coefficients

$$\begin{aligned}
Y_{uu\delta_r} &= -Y_{uvf} = \rho c_{L\alpha} S_{fin} \\
Z_{uu\delta_s} &= Z_{uvf} = -\rho c_{L\alpha} S_{fin} \\
Y_{urf} &= -Z_{uqf} = -\rho c_{L\alpha} S_{fin} x_{fin}
\end{aligned} \tag{3.24}$$

The set of equations which gives the fin moment coefficients are given below:

$$\begin{aligned}
M_{uu\delta_s} &= M_{uvf} = \rho c_{L\alpha} S_{fin} x_{fin} \\
N_{uu\delta_r} &= -N_{uvf} = -\rho c_{L\alpha} S_{fin} x_{fin} \\
M_{uqf} &= -N_{urf} = -\rho c_{L\alpha} S_{fin} x_{fin}^2
\end{aligned} \tag{3.25}$$

where,

$$\begin{aligned}
c_{L\alpha} &= \left( \frac{1}{2\alpha\pi} + \frac{1}{\pi(AR_e)} \right)^{-1} \\
AR_e &= 2. \left( \frac{b_{fin}^2}{S_{fin}} \right)
\end{aligned} \tag{3.26}$$

and

$\alpha$  is angle of attack.

Parameter	Value	Units	Description
$Y_{uu\delta_r}$	24.94	$kg/(m.rad)$	Fin Lift Force
$Y_{uvf}$	-24.94	$kg/m$	Fin Lift Force
$Z_{uu\delta_s}$	-24.94	$kg/(m.rad)$	Fin Lift Force
$Z_{uvf}$	-24.94	$kg/m$	Fin Lift Force
$Z_{uqf}$	-10.17	$kg/rad$	Fin Lift Force
$Y_{urf}$	10.17	$kg/rad$	Fin Lift Force
$M_{uu\delta_s}$	-10.17	$kg/rad$	Fin Lift Moment
$M_{uvf}$	-10.17	$kg$	Fin Lift Moment
$N_{uu\delta_r}$	-10.17	$kg/rad$	Fin Lift Moment
$N_{uvf}$	-10.17	$kg$	Fin Lift Moment
$M_{uqf}$	-4.1473	$kg.m/rad$	Fin Lift Moment
$N_{urf}$	-4.1473	$kg.m/rad$	Fin Lift Moment

Table 3.5: Fin lift coefficients

## 3.6 Propulsion Model

In general, propeller is considered as a constant source of thrust and torque. The values of the coefficients are derived from the design point of view and experimental point of view.

### 3.6.1 Propeller Thrust

The AUV is assumed to have a steady velocity and the propeller is maintained constant. So the parameter of Propeller thrust can be given by:

$$X_{prop} = -X_{u|u}|u| \quad (3.27)$$

### 3.6.2 Propeller Torque

The propeller torque is assumed to match with the hydrostatic roll moment since the AUV is running at a constant speed under steady state condition.

The parameter of Propeller thrust can be given by:

$$K_{prop} = -K_{HS} = (y_g W - y_b B) \cos \theta \cos \phi + (z_g W - z_b B) \cos \theta \sin \phi \quad (3.28)$$

Parameter	Value	Units	Description
$X_{prop}$	2.04	N	Propeller Thrust
$K_{prop}$	-0.3248	N-m	Propeller Torque

Table 3.6: Propeller parameter

### 3.7 Combined Terms

Combining the like terms from the added mass coefficients, body lift coefficients and fin lift parameter, we get the following combined coefficients:

$$\begin{aligned} Y_{uv} &= Y_{uwl} + Y_{uvf} \\ Y_{ur} &= Y_{ura} + Y_{urf} \\ Z_{uw} &= Z_{uwl} + Z_{uwf} \\ Z_{uq} &= Z_{uqa} + Z_{uqf} \\ M_{uw} &= M_{uwa} + M_{uwl} + M_{uwf} \\ M_{uq} &= M_{uqa} + M_{uqf} \\ N_{uv} &= N_{uva} + N_{uwl} + N_{uvf} \\ N_{ur} &= N_{ura} + N_{urf} \end{aligned} \tag{3.29}$$



# Chapter 4

## AUV Simulation

In this chapter, we have defined the equations administering the movement of the AUV. These equations consist of the following elements:

- Kinematics: the geometric aspects of motion
- Rigid-body Dynamics: the AUV inertia matrix
- Mechanics: forces and moments causing motion

These elements are addressed in the following sections.

### 4.1 AUV Kinematics

The movement of the body-fixed frame of reference is depicted in respect to an inertial or earth-fixed reference frame. The general movement of the AUV in six degrees of freedom can be depicted by the following vectors:

$$\begin{aligned}\eta_1 &= [x \ y \ z]^T \\ \eta_2 &= [\phi \ \theta \ \psi]^T \\ \nu_1 &= [u \ v \ w]^T \\ \nu_2 &= [p \ q \ r]^T \\ \tau_1 &= [X \ Y \ Z]^T \\ \tau_2 &= [K \ M \ N]^T\end{aligned}$$

where,  $\eta$  describes the position and orientation vector of the AUV with respect to the earth fixed reference frame,  $\nu$  the translational and rotational velocities of the AUV with respect to the body-fixed reference frame, and  $\tau$  the total forces and moments acting on the AUV with respect to the body-fixed reference frame.

The coordinate transform relating translational velocities between body-fixed and inertial or earth-fixed coordinates is given below:

$$\begin{bmatrix} \dot{x} \\ \dot{y} \\ \dot{z} \end{bmatrix} = J_1(\eta_2) \begin{bmatrix} u \\ v \\ w \end{bmatrix}$$

where

$$J_1(\eta_2) = \begin{bmatrix} \cos\psi\cos\theta & -\sin\psi\cos\phi + \cos\psi\sin\theta\sin\phi & \sin\psi\sin\phi + \cos\psi\sin\theta\cos\phi \\ \sin\psi\cos\theta & \cos\psi\cos\phi + \sin\psi\sin\theta\sin\phi & -\cos\psi\sin\phi + \sin\psi\sin\theta\cos\phi \\ -\sin\theta & \cos\theta\sin\phi & \cos\theta\cos\phi \end{bmatrix}$$

The below coordinate transform relates the rotational velocities between body-fixed and earth-fixed coordinates:

$$\begin{bmatrix} \dot{\phi} \\ \dot{\theta} \\ \dot{\psi} \end{bmatrix} = J_2(\eta_2) \begin{bmatrix} p \\ q \\ r \end{bmatrix}$$

where

$$J_2(\eta_2) = \begin{bmatrix} 1 & \sin\phi\tan\theta & \cos\phi\tan\theta \\ 0 & \cos\phi & -\sin\phi \\ 0 & \sin\phi/\cos\theta & \cos\phi/\cos\theta \end{bmatrix}$$

## 4.2 AUV Rigid-Body Dynamics

Vehicle centers of gravity and centers of buoyancy are defined in terms of the body-fixed coordinate system as follows:

$$r_g = [x_g \quad y_g \quad z_g]^T$$

$$r_b = [x_b \quad y_b \quad z_b]^T$$

Given that the body-fixed coordinate system centered at the vehicle center of buoyancy, the inertia tensor matrix is given as :

$$I_o = \begin{bmatrix} I_{xx} & 0 & 0 \\ 0 & I_{yy} & 0 \\ 0 & 0 & I_{zz} \end{bmatrix}$$

The origin of the body-fixed coordinate system is located at the center of buoyancy.

The following are the equations of motion for a rigid body in six degrees of freedom, defined with respect to body-fixed coordinate system:

$$m[\dot{u} - vr + wq - x_g(q^2 + r^2) + y_g(pq - \dot{r}) + z_g(pr + \dot{q})] = \sum X_{ext}$$

$$m[\dot{v} - wp + ur - y_g(r^2 + p^2) + z_g(qr - \dot{p}) + x_g(qp + \dot{r})] = \sum Y_{ext}$$

$$m[\dot{w} - uq + vp - z_g(p^2 + q^2) + x_g(rp - \dot{q}) + y_g(rq + \dot{p})] = \sum Z_{ext}$$

$$I_{xx}\dot{p} + (I_{zz} - I_{yy})qr + m[y_g(\dot{w} - uq + vp) - z_g(\dot{v} - wp + ur)] = \sum K_{ext}$$

$$I_{yy}\dot{q} + (I_{xx} - I_{zz})rp + m[z_g(\dot{u} - vr + wq) - x_g(\dot{w} - uq + vp)] = \sum M_{ext}$$

$$I_{zz}\dot{r} + (I_{yy} - I_{xx})pq + m[x_g(\dot{v} - wp + ur) - y_g(\dot{u} - vr + wq)] = \sum N_{ext}$$

where  $m$  is the mass of the AUV.

### 4.3 Hydrostatics

The AUV experiences hydrostatic forces and moments on account of the combined impacts of the weight of the AUV and buoyancy on the vehicle. The forces and moments are expressed with respect to body-fixed coordinate system.

The following are the nonlinear equations for hydrostatic forces and moments:

$$\begin{aligned}
 X_{HS} &= -(W - B)\sin\theta \\
 Y_{HS} &= -(W - B)\cos\theta\sin\phi \\
 X_{HS} &= -(W - B)\cos\theta\cos\phi \\
 K_{HS} &= -(y_g W - y_b B)\cos\theta\cos\phi - (z_g W - z_b B)\cos\theta\sin\phi \\
 M_{HS} &= -(z_g W - z_b B)\sin\theta - (x_g W - x_b B)\cos\theta\cos\phi \\
 N_{HS} &= -(x_g W - x_b B)\cos\theta\sin\phi - (y_g W - y_b B)\sin\theta
 \end{aligned}$$

### 4.4 AUV Forces and Moments

The forces and moments acting on the AUV in six degrees of freedom is given by the following equations:

$$\begin{aligned}
 \sum X_{ext} &= X_{HS} + X_{u|u}|u| + X_{\dot{u}}\dot{u} + X_{wq}wq + X_{qq}qq + X_{vr}vr + X_{prop} \\
 \sum Y_{ext} &= Y_{HS} + Y_{v|v}|v| + Y_{r|r}|r| + Y_{\dot{v}}\dot{v} + Y_{\dot{r}}\dot{r} + Y_{ur}ur + Y_{wp}wp \\
 &\quad + Y_{pq}pq + Y_{uv}uv + Y_{uu\delta_r}u^2\delta_r \\
 \sum Z_{ext} &= Z_{HS} + Z_{w|w}|w| + Z_{q|q}|q| + Z_{\dot{w}}\dot{w} + Z_{\dot{q}}\dot{q} + Z_{uq}uq + Z_{vp}vp \\
 &\quad + Z_{rp}rp + Z_{uw}uw + Z_{uu\delta_s}u^2\delta_s \\
 \sum K_{ext} &= K_{HS} + K_{p|p}|p| + K_{\dot{p}}\dot{p} + K_{prop} \\
 \sum M_{ext} &= M_{HS} + M_{w|w}|w| + M_{q|q}|q| + M_{\dot{w}}\dot{w} + M_{\dot{q}}\dot{q} + M_{uq}uq \\
 &\quad + M_{vp}vp + M_{rp}rp + M_{uw}uw + M_{uu\delta_s}u^2\delta_s \\
 \sum N_{ext} &= N_{HS} + N_{v|v}|v| + N_{r|r}|r| + N_{\dot{v}}\dot{v} + N_{\dot{r}}\dot{r} + N_{ur}ur + N_{wp}wp \\
 &\quad + N_{pq}pq + N_{uv}uv + N_{uu\delta_r}u^2\delta_r
 \end{aligned}$$

## 4.5 Combined Nonlinear Equations of Motion

After combining the equations of the AUV rigid-body dynamics and the equations of the forces and moments acting on the AUV, we can get the combined nonlinear equations of motion in six degrees of freedom for our AUV.

SURGE (Translation along X-axis)

$$\begin{aligned} & m[\dot{u} - vr + wq - x_g(q^2 + r^2) + y_g(pq - \dot{r}) + z_g(pr + \dot{q})] \\ & = X_{HS} + X_{u|u}|u| + X_{\dot{u}}\dot{u} + X_{wq}wq + X_{qq}qq + X_{vr}vr + X_{prop} \end{aligned}$$

SWAY (Translation along Y-axis)

$$\begin{aligned} & m[\dot{v} - wp + ur - y_g(r^2 + p^2) + z_g(qr - \dot{p}) + x_g(qp + \dot{r})] \\ & = Y_{HS} + Y_{v|v}|v| + Y_{r|r}|r| + Y_{\dot{v}}\dot{v} + Y_{\dot{r}}\dot{r} + Y_{ur}ur + Y_{wp}wp \\ & \quad + Y_{pq}pq + Y_{uv}uv + Y_{uu\delta_r}u^2\delta_r \end{aligned}$$

HEAVE (Translation along Z-axis)

$$\begin{aligned} & m[\dot{w} - uq + vp - z_g(p^2 + q^2) + x_g(rp - \dot{q}) + y_g(rq + \dot{p})] \\ & = Z_{HS} + Z_{w|w}|w| + Z_{q|q}|q| + Z_{\dot{w}}\dot{w} + Z_{\dot{q}}\dot{q} + Z_{uq}uq + Z_{vp}vp \\ & \quad + Z_{rp}rp + Z_{uw}uw + Z_{uu\delta_s}u^2\delta_s \end{aligned}$$

ROLL (Rotation about X-axis)

$$\begin{aligned} & I_{xx}\dot{p} + (I_{zz} - I_{yy})qr + m[y_g(\dot{w} - uq + vp) - z_g(\dot{v} - wp + ur)] \\ & = K_{HS} + K_{p|p}|p| + K_{\dot{p}}\dot{p} + K_{prop} \end{aligned}$$

PITCH (Rotation about Y-axis)

$$\begin{aligned} & I_{yy}\dot{q} + (I_{xx} - I_{zz})rp + m[z_g(\dot{u} - vr + wq) - x_g(\dot{w} - uq + vp)] \\ & = M_{HS} + M_{w|w}|w| + M_{q|q}|q| + M_{\dot{w}}\dot{w} + M_{\dot{q}}\dot{q} + M_{uq}uq \\ & \quad + M_{vp}vp + M_{rp}rp + M_{uw}uw + M_{uu\delta_s}u^2\delta_s \end{aligned}$$

YAW (Rotation about Z-axis)

$$\begin{aligned} & I_{zz}\dot{r} + (I_{yy} - I_{xx})pq + m[x_g(\dot{v} - wp + ur) - y_g(\dot{u} - vr + wq)] \\ & = N_{HS} + N_{v|v}|v| + N_{r|r}|r| + N_{\dot{v}}\dot{v} + N_{\dot{r}}\dot{r} + N_{ur}ur + N_{wp}wp \\ & \quad + N_{pq}pq + N_{uv}uv + N_{uu\delta_r}u^2\delta_r \end{aligned}$$

After separating the acceleration terms from the other terms in the AUV equations of motion, it can be summarized in the matrix form as follows:

$$\begin{bmatrix} m - X_{\dot{u}} & 0 & 0 & 0 & mz_g & -my_g \\ 0 & m - Y_{\dot{v}} & 0 & -mz_g & 0 & mx_g - Y_{\dot{r}} \\ 0 & 0 & m - Z_{\dot{w}} & my_g & -mx_g - Z_{\dot{q}} & 0 \\ 0 & -mz_g & my_g & I_{xx} - K_{\dot{p}} & 0 & 0 \\ mz_g & 0 & -mx_g - M_{\dot{w}} & 0 & I_{yy} - M_{\dot{q}} & 0 \\ -my_g & mx_g - N_{\dot{v}} & 0 & 0 & 0 & I_{zz} - N_{\dot{r}} \end{bmatrix} \begin{bmatrix} \dot{u} \\ \dot{v} \\ \dot{w} \\ \dot{p} \\ \dot{q} \\ \dot{r} \end{bmatrix} = \begin{bmatrix} \sum X \\ \sum Y \\ \sum Z \\ \sum K \\ \sum M \\ \sum N \end{bmatrix}$$

This implies,

$$\begin{bmatrix} \dot{u} \\ \dot{v} \\ \dot{w} \\ \dot{p} \\ \dot{q} \\ \dot{r} \end{bmatrix} = \begin{bmatrix} m - X_{\dot{u}} & 0 & 0 & 0 & mz_g & -my_g \\ 0 & m - Y_{\dot{v}} & 0 & -mz_g & 0 & mx_g - Y_{\dot{r}} \\ 0 & 0 & m - Z_{\dot{w}} & my_g & -mx_g - Z_{\dot{q}} & 0 \\ 0 & -mz_g & my_g & I_{xx} - K_{\dot{p}} & 0 & 0 \\ mz_g & 0 & -mx_g - M_{\dot{w}} & 0 & I_{yy} - M_{\dot{q}} & 0 \\ -my_g & mx_g - N_{\dot{v}} & 0 & 0 & 0 & I_{zz} - N_{\dot{r}} \end{bmatrix}^{-1} \begin{bmatrix} \sum X \\ \sum Y \\ \sum Z \\ \sum K \\ \sum M \\ \sum N \end{bmatrix}$$

## 4.6 Numerical Integration of the Equations of Motion

The non-linear differential equations of the AUV rigid-body dynamics and the equations of the forces and moments acting on the AUV which give us the AUV accelerations in the different reference frames. Because of the complex and highly non-linear nature of these equations, numerical integration is used to solve for the AUV speed and position in time.

Let at each time step we can express the above equation as:

$$\dot{x}_n = f(x_n, u_n)$$

where,  $x$  is the state vector of the AUV consisting of position, orientation, translational velocities and rotational velocities.

and  $u$  is the input vector.

$$u = [\delta_s \quad \delta_r \quad X_{prop} \quad K_{prop}]^T$$

Runge-Kutta Method is one of the most accurate method of numerical integration.

### 4.6.1 Runge-Kutta Method

This method is one of the most accurate method since it averages the slope at four points. We first calculate the following:

$$\begin{aligned} k_1 &= f(x_n, u_n) \\ k_2 &= f\left(x_n + \frac{h}{2}, u_n + \frac{k_1}{2}\right) \\ k_3 &= f\left(x_n + \frac{h}{2}, u_n + \frac{k_2}{2}\right) \\ k_4 &= f(x_n + h, u_n + k_3) \end{aligned}$$

After combining the above equations, the updation is done by the below formulae:

$$y_{n+1} = y_n + \frac{h}{6}[k_1 + 2k_2 + 2k_3 + k_4]$$

where,  $h$  is the time step size.

## 4.7 AUV Simulation Results

The above numerical integration method was implemented in MATLAB using the derived parameter and the initial conditions. The forces and moments (which is a function of the AUV speed and position) acting on the AUV is calculated for each time step. These forces is used to determine the AUV acceleration and then these acceleration are approximated to find the new AUV velocities, which acts as inputs for the next time step.

Inputs required by the AUV:

- *Initial Conditions*, initial value of AUV state vector.
- *Control Inputs*, stern angle and rudder angle inputs for the fin control.

Results of the AUV simulation for different stern and rudder angles are given below:

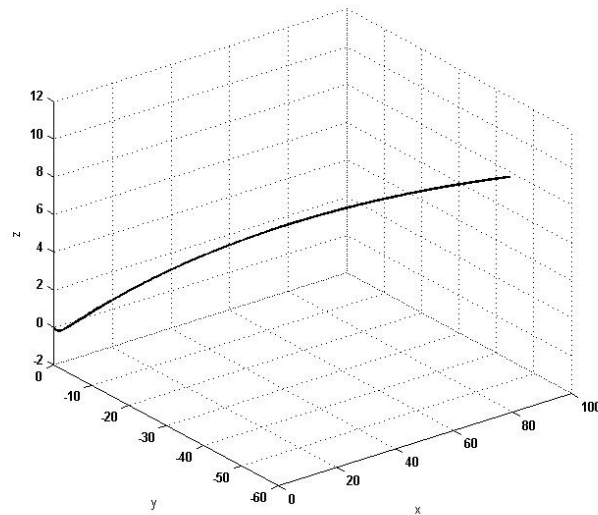


Figure 4.1: AUV Motion in XYZ plane for stern angle= $0^\circ$  and rudder angle= $0^\circ$

From the figures we can observe that the AUV due to it's inherent non-linear characteristics does not follow a straight path even when the inputs to the control surfaces is zero. This can be attributed to the fact that the AUV does not have equal weight and buoyancy as well as the AUV's weight distribution is non-uniform leading to difference in response of the AUV to the inputs of rudder and stern control fins. Therefore, for accurate trajectory tracking system we require a continuous control signal to cancel out the effects of these non-linearities. Thus, a controller is an integral part of the AUV.

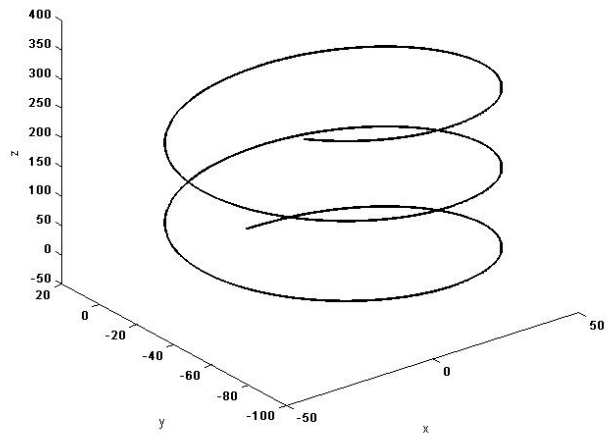


Figure 4.2: AUV Motion in XYZ plane for stern angle=30° and rudder angle=0°

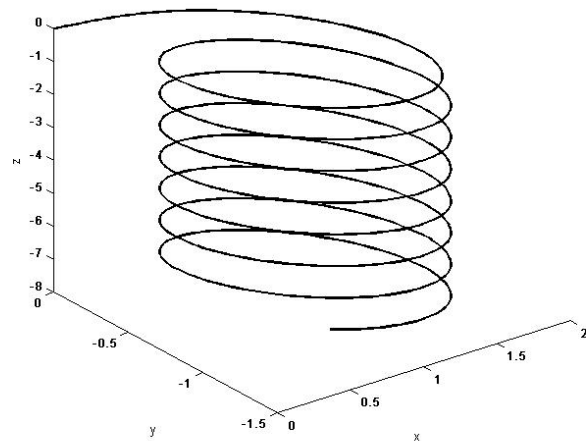


Figure 4.3: AUV Motion in XYZ plane for stern angle=0° and rudder angle=30°

# Chapter 5

## Linearised Depth Plane and Heading Plane Model of the AUV

This chapter describes the process by which we can linearise and decouple the AUV model to create a three degree of freedom based Heading Plane Model and three degree of freedom Depth Plane Model. This will help us to better visualise, the AUV response in the to different planes of motion, thereby increasing the accuracy of the AUV controller design.

An important assumption taken in the derivation of these models is the constant forward speed motion of the AUV, at a speed of  $U = 1.25m/s = 2.5knots$ .

### 5.1 Depth Plane Model

While considering the motion of the AUV in the depth plane, we will only consider the body relative surge velocity,  $u$ , heave velocity,  $w$ , pitch rate,  $q$  as well as earth frame referenced, position  $x$ , depth  $z$  and pitch angle  $\theta$ . All other body relative velocity and earth frame position parameters are considered zero, i.e.  $v = p = r = y = \phi = \psi = 0$ .

Moreover, since we have assumed a constant speed motion of the AUV, system is linearised along the considering only small perturbations to the AUV,  $u = U + u'$ ,  $w = w'$  and  $q = q'$ .

#### 5.1.1 AUV Kinematics

Applying above assumptions,

$$\begin{aligned}\dot{x} &= u \cos \theta + w \sin \theta \\ \dot{z} &= -u \sin \theta + w \cos \theta \\ \dot{\theta} &= q\end{aligned}\tag{5.1}$$

Further considering only small perturbations, the equations are further reduced to,

$$\begin{aligned}\dot{x} &= u + w\theta \\ \dot{z} &= -U\theta + w \\ \dot{\theta} &= q\end{aligned}\tag{5.2}$$



### 5.1.2 AUV Dynamics

The AUV dynamic equations considering all the assumptions, additionally eliminating all the smaller terms, are reduced to

$$\begin{aligned}\sum X &= m[\dot{u} + z_g \dot{q}] \\ \sum Z &= m[\dot{w} - x_g \dot{q} - Uq] \\ \sum M &= I_{yy} \dot{q} + m[z_g \dot{u} - x_g(\dot{w} - Uq)]\end{aligned}\tag{5.3}$$

### 5.1.3 Linearised AUV parameter Derivation

AUV coefficients derived in previous sections were based on non-linear equations. But, with the assumptions made, there is a slight difference in the formula for the derivation of the coefficients. These have been given below,

#### Hydrostatic Forces

Taking the above assumptions and dropping the higher order terms as well as any constant term, hydrostatic forces are linearised to,

$$\begin{aligned}X_\theta &= -(W - B)\theta \\ M_\theta &= -(z_g W - z_b B)\theta\end{aligned}\tag{5.4}$$

#### Axial Drag

Axial Drag of the AUV is expressed as,

$$X = -\frac{1}{2}\rho C_d A_f (U + u')|U + u'|\tag{5.5}$$

Since,  $u'$  is very much less than  $U$ , from the above equation  $X_u$  is reduced to,

$$X_u = -\rho C_d A_f U = X_{u|u} * 2U\tag{5.6}$$

#### AUV cross-flow drag

In order to linearise the AUV cross-flow drag coefficients, heave velocity as well as pitch perturbations need to be linearised around zero. This can be done by approximating the quadratic heave and pitch perturbations as a linear function, i.e.

$$\begin{aligned}w^2 &= m_w w = 0.1231w \\ q^2 &= m_q q = 0.0108q\end{aligned}\tag{5.7}$$

$$\begin{aligned}Z_{wc} &= Z_{ww} m_w \\ M_{wc} &= M_{ww} m_w \\ Z_{qc} &= Z_{qq} m_q \\ M_{qc} &= M_{qq} m_q\end{aligned}\tag{5.8}$$

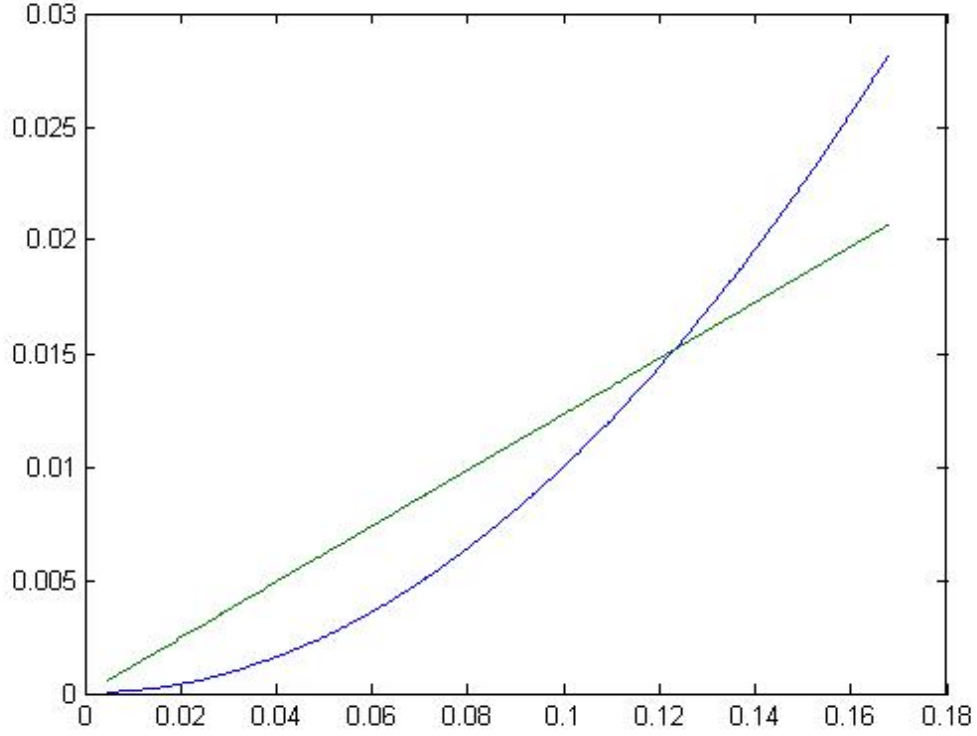


Figure 5.1: Velocity squared vs. Velocity

### Added Mass Terms

From the previous sections, it is seen that the axial added mass terms and cross-flow added mass terms do not depend only on the mass density of water sticking to the surface of the AUV. Thus, they remain same. Remaining crossterms, which depend on the velocity of the AUV, are modified as follows,

$$\begin{aligned}
 X_{qa} &= Z_{\dot{q}}m_q \\
 Z_{qa} &= -X_{\dot{u}}U \\
 M_{wa} &= -(Z_{\dot{w}} - X_{\dot{u}})U \\
 M_{qa} &= -Z_{\dot{q}}U
 \end{aligned} \tag{5.9}$$

### Body Lift Force and Moment

Modified Body Lift parameter and Body Lift Moment as obtained from the modified equation of AUV body lift is,

$$\begin{aligned}
 Z_L &= -\frac{1}{2}\rho d^2 C_{yd\beta} U w \\
 Z_{wl} &= -\frac{1}{2}\rho d^2 C_{yd\beta} U \\
 M_{wl} &= -\frac{1}{2}\rho d^2 C_{yd\beta} x_{cp} U
 \end{aligned} \tag{5.10}$$

## Fin Lift

Fin Lift Coefficients are modified as follows,

$$\begin{aligned} Z_{\delta s} &= -\rho C_{L\alpha} S_{fin} U^2 \\ Z_{wf} &= -\frac{1}{2} \rho C_{L\alpha} S_{fin} U \\ Z_{qf} &= \frac{1}{2} \rho C_{L\alpha} S_{fin} x_{fin} U \end{aligned} \quad (5.11)$$

Fin Moment coefficients,

$$\begin{aligned} M_{\delta s} &= \rho C_{L\alpha} S_{fin} x_{fin} U^2 \\ Z_{wf} &= \frac{1}{2} \rho C_{L\alpha} S_{fin} x_{fin} U \\ Z_{qf} &= -\frac{1}{2} \rho C_{L\alpha} S_{fin} (x_{fin})^2 U \end{aligned} \quad (5.12)$$

## Total depth plane Forces and Moments

The total forces and moment experienced by the body while in depth plane motion, is given by

$$\begin{aligned} \sum X &= X_{\dot{u}} \dot{u} + X_u u + X_q q + X_\theta \\ \sum Z &= Z_{\dot{w}} \dot{w} + Z_{\dot{q}} \dot{q} + Z_w w + Z_q q + Z_{\delta s} \delta_s \\ \sum M &= M_{\dot{w}} \dot{w} + M_{\dot{q}} \dot{q} + M_w w + M_q q + M_\theta + M_{\delta s} \delta_s \end{aligned} \quad (5.13)$$

where, the combined terms are given as,

$$\begin{aligned} Z_w &= Z_{wc} + Z_{wl} + Z_{wf} \\ M_w &= M_{wc} + M_{wa} + M_{wl} + M_{wf} \\ Z_q &= Z_{qc} + Z_{qa} + Z_{qf} \\ M_q &= M_{qc} + M_{qa} + M_{qf} \end{aligned} \quad (5.14)$$

## Value of Linearised parameter

From the above mentioned formulae, we arrived at the following values of the linearised parameter,

Parameter	Value	Unit	Description
$X_{\dot{u}}$	-0.57858	$kg$	Added Mass
$Z_w$	-45.225	$kg/s$	Combined Term
$Z_q$	-5.64372	$kg - m/s$	Combined Term
$Z_{\dot{w}}$	-24.0189	$kg$	Added Mass
$Z_{\dot{q}}$	2.2586	$kg - m$	Added Mass
$Z_{\delta s}$	-38.96875	$kg - m/s^2$	Fin Lift
$M_\theta$	-3.49236	$kg - m^2/s^2$	Hydrostatic Force
$M_w$	19.9192	$kg - m/s$	Combined Term
$M_q$	-5.4198	$kg - m^2/s$	Combined Term
$M_{\dot{w}}$	2.2586	$kg - m$	Added Mass
$M_{\dot{q}}$	-2.344	$kg - m^2$	Added Mass
$M_{\delta s}$	-15.8906	$kg - m^2/s^2$	Fin Lift

Table 5.1: Value of Linearised Coefficients

### 5.1.4 Linearised and Decoupled Equation of Motion of AUV in Depth Plan

Taking into account the assumptions made at the beginning of the chapter, the linearised and decoupled equation of motion of the AUV in depth plane model is,

$$\begin{aligned}
 \dot{w} - [mx_g + Z_{\dot{q}}]\dot{q} - Z_w w - [mU + Z_q]q &= Z_{\delta_s}\delta_s \\
 -[mx_g + M_{\dot{w}}]\dot{w} + [I_{yy} - M_{\dot{q}}]\dot{q} - M_w w + [mx_g U - M_q]q - M_{\theta} &= M_{\delta_s}\delta_s \\
 \dot{Z} &= w - U\theta \\
 \dot{\theta} &= q
 \end{aligned} \tag{5.15}$$

Thus, the above equation in state space form, considering  $w$  is very very small, is,

$$\begin{bmatrix} (I_{yy} - M_{\dot{q}}) & 0 & 0 \\ 0 & 1 & 0 \\ 0 & 0 & 1 \end{bmatrix} \begin{bmatrix} \dot{q} \\ \dot{Z} \\ \dot{\theta} \end{bmatrix} - \begin{bmatrix} (-mx_g U + m_q) & 0 & 0 \\ 0 & 0 & -U \\ 1 & 0 & 0 \end{bmatrix} \begin{bmatrix} q \\ Z \\ \theta \end{bmatrix} = \begin{bmatrix} M_{\delta_s} \\ 0 \\ 0 \end{bmatrix} \delta_s \tag{5.16}$$

Further simplifying the above equation we get the 3 term state space representation of the Depth Plane Model of the AUV,

$$\begin{bmatrix} \dot{q} \\ \dot{\theta} \\ \dot{Z} \end{bmatrix} = \begin{bmatrix} -1.5005 & -0.9669 & 0 \\ 1 & 0 & 0 \\ 0 & -1.25 & 0 \end{bmatrix} \begin{bmatrix} q \\ \theta \\ Z \end{bmatrix} + \begin{bmatrix} -4.3994 \\ 0 \\ 0 \end{bmatrix} \delta_s \tag{5.17}$$

## 5.2 Heading Plane Model

Similar procedure is followed as before, to find the heading plane model of the AUV. While considering the motion of the AUV in the heading plane, we will only consider the body relative surge velocity,  $u$ , sway velocity,  $v$ , yaw rate,  $r$  as well as earth frame referenced, position  $x$ ,  $y$  and yaw angle  $\psi$ . All other body relative velocity and earth frame position parameters are considered zero, i.e.  $w = p = q = z = \phi = \theta = 0$ .

Moreover, since we have assumed a constant speed motion of the AUV, system is linearised along the considering only small perturbations to the AUV,  $u = U + u'$ ,  $v = v'$  and  $r = r'$ .

### 5.2.1 AUV Kinematics

Applying above assumptions,

$$\begin{aligned}
 \dot{x} &= u \cos \psi - v \sin \psi \\
 \dot{y} &= -u \sin \psi + v \cos \psi \\
 \dot{\psi} &= r
 \end{aligned} \tag{5.18}$$

Further considering only small perturbations, the equations are further reduced to,

$$\begin{aligned}\dot{x} &= u + v\psi \\ \dot{y} &= U\psi + v \\ \dot{\psi} &= r\end{aligned}\tag{5.19}$$

### 5.2.2 AUV Dynamics

The AUV dynamic equations considering all the assumptions, additionally eliminating all the smaller terms, are reduced to

$$\begin{aligned}\sum X &= m[\dot{u} - vr - x_g r^2] \\ \sum Y &= m[\dot{v} + x_g \dot{r} + Ur] \\ \sum N &= I_{zz} \dot{r} + m[x_g \dot{v} + x_g Ur]\end{aligned}\tag{5.20}$$

### 5.2.3 Linearised AUV parameter Derivation

AUV coefficients derived in previous sections were based on non-linear equations. But, with the assumptions made, there is a slight difference in the formula for the derivation of the coefficients. These have been given below,

#### Hydrostatic Forces

Taking the above assumptions and dropping the higher order terms as well as any constant term, hydrostatic forces are linearised to,

$$\begin{aligned}X_{HS} &= 0 \\ Y_{HS} &= 0 \\ N_{HS} &= 0\end{aligned}\tag{5.21}$$

#### Axial Drag

Axial Drag of the AUV is expressed as,

$$X = -\frac{1}{2}\rho C_d A_f (U + u')|U + u'|\tag{5.22}$$

Since,  $u'$  is very much less than  $U$ , from the above equation  $X_u$  is reduced to,

$$X_u = -\rho C_d A_f U = X_{u|u} * 2U\tag{5.23}$$

#### AUV cross-flow drag

In order to linearise the AUV cross-flow drag coefficients, heave velocity as well as pitch perturbations need to be linearised around zero. This can be done by approximating the quadratic heave and pitch perturbations as a linear function, i.e.

$$\begin{aligned}v^2 &= m_v v = 0.0633v \\ r^2 &= m_r r = 0.042r\end{aligned}\tag{5.24}$$

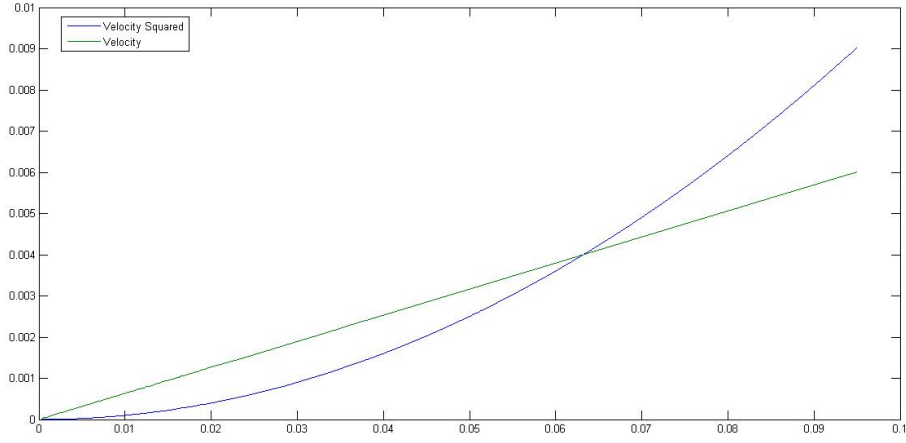


Figure 5.2: Velocity squared vs. Velocity

$$\begin{aligned}
Y_{vc} &= Y_{vv}m_v \\
Y_{rc} &= Y_{rr}m_r \\
N_{vc} &= N_{vv}m_v \\
N_{rc} &= N_{rr}m_r
\end{aligned} \tag{5.25}$$

### Added Mass Terms

From the previous sections, it is seen that the axial added mass terms and cross-flow added mass terms do not depend only on the mass density of water sticking to the surface of the AUV. Thus, they remain same. Remaining crossterms, which depend on the velocity of the AUV, are modified as follows,

$$\begin{aligned}
X_{ra} &= -Y_{\dot{r}}m_r \\
Y_{ra} &= X_{\dot{u}}U \\
N_{va} &= -(X_{\dot{u}} - Y_{\dot{v}})U \\
N_{ra} &= Y_{\dot{r}}U
\end{aligned} \tag{5.26}$$

### Body Lift Force and Moment

Modified Body Lift parameter and Body Lift Moment as obtained from the modified equation of AUV body lift is,

$$\begin{aligned}
Y_{vl} &= -\frac{1}{2}\rho d^2 C_{yd\beta} U \\
N_{vl} &= \frac{1}{2}\rho d^2 C_{yd\beta} x_{cp} U
\end{aligned} \tag{5.27}$$

## Fin Lift

Fin Lift Coefficients are modified as follows,

$$\begin{aligned}
 Y_{\delta r} &= \rho C_{L\alpha} S_{fin} U^2 \\
 Y_{vf} &= -\frac{1}{2} \rho C_{L\alpha} S_{fin} U \\
 Y_{rf} &= -\frac{1}{2} \rho C_{L\alpha} S_{fin} x_{fin} U
 \end{aligned} \tag{5.28}$$

Fin Moment coefficients,

$$\begin{aligned}
 N_{\delta r} &= \rho C_{L\alpha} S_{fin} x_{fin} U^2 \\
 N_{vf} &= -\frac{1}{2} \rho C_{L\alpha} S_{fin} x_{fin} U \\
 N_{rf} &= -\frac{1}{2} \rho C_{L\alpha} S_{fin} (x_{fin})^2 U
 \end{aligned} \tag{5.29}$$

## Total depth plane Forces and Moments

The total forces and moment experienced by the body while in depth plane motion, is given by

$$\begin{aligned}
 \sum X &= X_{\dot{u}} \dot{u} + X_u u + X_r r \\
 \sum Y &= Y_{\dot{r}} \dot{r} + Y_{\dot{v}} \dot{v} + Y_r r + Y_v v + Y_{\delta r} \delta_r \\
 \sum N &= N_{\dot{r}} \dot{r} + N_{\dot{v}} \dot{v} + N_r r + N_v v + N_{\delta r} \delta_r
 \end{aligned} \tag{5.30}$$

where, the combined terms are given as,

$$\begin{aligned}
 Y_v &= Y_{vc} + Y_{vl} + Y_{vf} \\
 N_v &= N_{vc} + N_{va} + N_{vl} + N_{vf} \\
 Y_r &= Y_{rc} + Y_{ra} + Y_{rf} \\
 N_r &= N_{rc} + N_{ra} + N_{rf}
 \end{aligned} \tag{5.31}$$

## Value of Linearised parameter

From the above mentioned formulae, we arrived at the following values of the linearised parameter,

Parameter	Value	Unit	Description
$X_{\dot{u}}$	-0.57858	$kg$	Added Mass
$Y_v$	-39.78196	$kg/s$	Combined Term
$Y_r$	-5.6747	$kg - m/s$	Combined Term
$Y_{\dot{v}}$	-24.0189	$kg$	Added Mass
$Y_{\dot{r}}$	-2.2586	$kg - m$	Added Mass
$Y_{\delta r}$	38.96875	$kg - m/s^2$	Fin Lift
$N_{HS}$	0	$kg - m^2/s^2$	Hydrostatic Force
$N_v$	-19.7976	$kg - m/s$	Combined Term
$N_r$	-5.43284	$kg - m^2/s$	Combined Term
$N_{\dot{v}}$	-2.2586	$kg - m$	Added Mass
$N_{\dot{r}}$	-2.344	$kg - m^2$	Added Mass
$N_{\delta r}$	-15.8906	$kg - m^2/s^2$	Fin Lift

Table 5.2: Value of Linearised Coefficients

## 5.2.4 Linearised and Decoupled Equation of Motion of AUV in Heading Plane

Taking into account the assumptions made at the beginning of the chapter, the linearised and decoupled equation of motion of the AUV in heading plane model is,

$$\begin{aligned}
 \dot{v} + [mx_g - Y_{\dot{r}}]\dot{r} - Y_v v + [mU + Y_r]r &= Y_{\delta r} \delta_r \\
 [mx_g - N_{\dot{v}}]\dot{v} + [I_{zz} - N_{\dot{r}}]\dot{r} - N_v v + [mx_g U - N_r]r &= N_{\delta r} \delta_r \\
 \dot{y} &= v + U\psi \\
 \dot{\psi} &= r
 \end{aligned} \tag{5.32}$$

Thus, the above equation in state space form, considering  $y$  is very very small, is,

$$\begin{bmatrix} (m - Y_{\dot{v}}) & -Y_{\dot{r}} & 0 \\ -N_{\dot{v}} & (I_{zz} - N_{\dot{r}}) & 0 \\ 0 & 0 & 1 \end{bmatrix} \begin{bmatrix} \dot{v} \\ \dot{r} \\ \dot{\psi} \end{bmatrix} - \begin{bmatrix} -Y_v & -(Y_r - mU) & 0 \\ -N_v & -N_r & 0 \\ 0 & 1 & 0 \end{bmatrix} \begin{bmatrix} v \\ r \\ \psi \end{bmatrix} = \begin{bmatrix} Y_{\delta r} \\ N_{\delta r} \\ 0 \end{bmatrix} \delta_r \tag{5.33}$$

Further simplifying the above equation we get the 3 term state space representation of the Heading Plane Model of the AUV,

$$\begin{bmatrix} \dot{v} \\ \dot{r} \\ \dot{\psi} \end{bmatrix} = \begin{bmatrix} -0.6782 & -0.3261 & 0 \\ -5.0571 & -1.3002 & 0 \\ 0 & 1 & 0 \end{bmatrix} \begin{bmatrix} v \\ r \\ \psi \end{bmatrix} + \begin{bmatrix} 1.2103 \\ -5.1563 \\ 0 \end{bmatrix} \delta_s \tag{5.34}$$



# Chapter 6

## Controller Design for Path Following Task

The main aim of the controller in the AUV is to make sure that the trajectory followed by the AUV is accurate and within the specified error band, so that the AUV completes its mission objectives with least cost and without any damage while it follows the predefined path. As seen in the previous chapter, due to the inherent properties of the AUV it is unable to even move in a straight line path, when there are no input to the control surfaces. Therefore, in order to track the trajectory accurately, constant inputs to the control surfaces based on current state of the system as well as the future state are required. To achieve this, we have decided to split the controller design problem in two parts, viz. one for heading plane and one for depth plane control. This provides a greater level of flexibility to the system, in terms of energy expended, as at any given particular time either both or only one controller may be used depending on the scenario leading to a greater savings in terms of energy requirement of the system. Moreover, this approach allows us to model the controllers more accurately based on the required dynamic behaviour of each control plane. In this chapter, we have first shown the responses of each control plane separately, without any controllers and then we have moved on to show the responses of the system with the use of Sliding Mode Controller.

### 6.1 Reponse of the system without any controller

In this section we have shown the response of the heading plane and depth plane system derived in the previous chapter without the use of a controller.

#### 6.1.1 Depth Plane System

The state space system derived in the previous chapter is as follows,

$$\begin{bmatrix} \dot{q} \\ \dot{\theta} \\ \dot{Z} \end{bmatrix} = \begin{bmatrix} -1.5005 & -0.9669 & 0 \\ 1 & 0 & 0 \\ 0 & -1.25 & 0 \end{bmatrix} \begin{bmatrix} q \\ \theta \\ Z \end{bmatrix} + \begin{bmatrix} -4.3994 \\ 0 \\ 0 \end{bmatrix} \delta_s \quad (6.1)$$

The poles of the system is given by eigenvalues of A, i.e. the poles of the system are  $[0, -0.7506 + j0.6356, -0.7506 - j0.6356]$

To check the controllability of the system we find the rank of the matrix  $U = [B|AB|A^2B]$

$$U = \begin{bmatrix} -4.3994 & 6.6013 & -5.6516 \\ 0 & -4.3994 & 6.6013 \\ 0 & 0 & 5.4992 \end{bmatrix}$$

Rank of  $U = 3$

Thus, from the above analysis we find that the depth plane model of the sys-

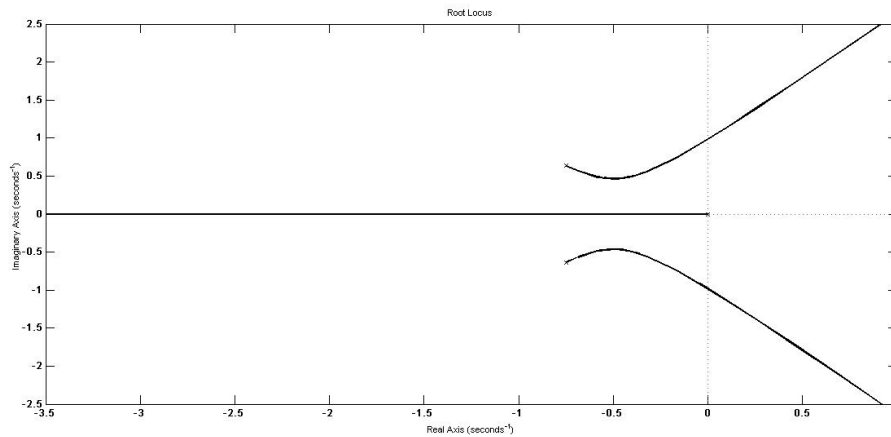


Figure 6.1: Root Locus Plot of the Depth Plane System

tem is *stable* as well as *controllable*. However the system response as observed below is not upto the desired standard. The system response is slow and unable to track the desired depth.

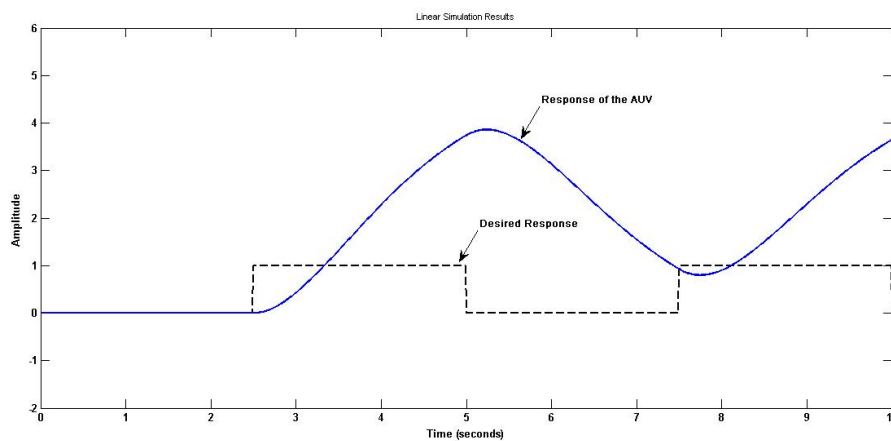


Figure 6.2: Response of the Depth Plane system (Depth vs. time)

## 6.1.2 Heading Plane System

The state space system derived in the previous chapter is as follows,

$$\begin{bmatrix} \dot{v} \\ \dot{r} \\ \dot{\psi} \end{bmatrix} = \begin{bmatrix} -0.6782 & -0.3261 & 0 \\ -5.0571 & -1.3002 & 0 \\ 0 & 1 & 0 \end{bmatrix} \begin{bmatrix} v \\ r \\ \psi \end{bmatrix} + \begin{bmatrix} 1.2103 \\ -5.1563 \\ 0 \end{bmatrix} \delta_s \quad (6.2)$$

The poles of the system is given by eigenvalues of A,i.e. the poles of the system are  $[0, -2.3105, 0.3322]$  To check the controllability of the system we find the rank of the matrix  $U = [B|AB|A^2B]$

$$U = \begin{bmatrix} 1.2103 & 0.8608 & -0.7741 \\ -5.1563 & 0.5834 & -5.1119 \\ 0 & -5.1563 & 0.5834 \end{bmatrix}$$

Rank of  $U = 3$

Thus, from the above analysis we find that the heading plane model of the system

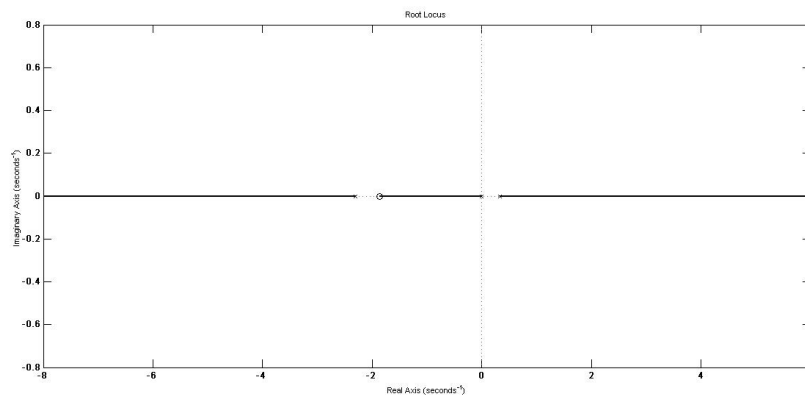


Figure 6.3: Root Locus Plot of the Heading Plane System

is *unstable* but *controllable*. However the system response as observed below is not of the desired standard. The system response is slow and unable to track the desired yaw angle ( $\psi$ ). The system response moreover diverges.

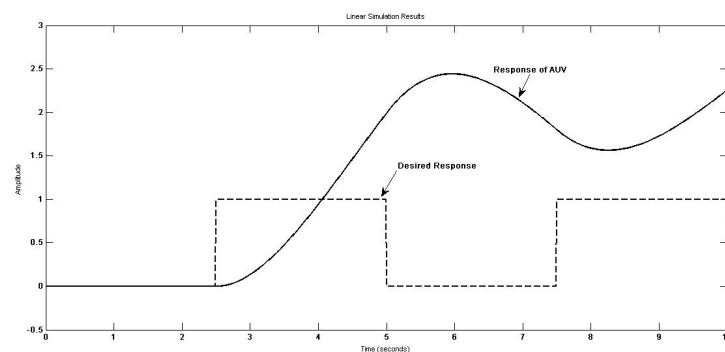


Figure 6.4: Response of the Heading Plane system (Heading ( $\psi$ ) vs. time)

## 6.2 Sliding Mode Controller (SMC)

From the simulations of the previous sections it can be seen that the system response is unsatisfactory and the AUV is not able to track the specified trajectory. Therefore, Sliding Mode Controller (SMC) is chosen for the purpose of controlling the AUV.

SMC is a switching discrete controller, which can control the system by altering the dynamic behavior of the system through the use of discrete control law. SMC can work with both continuous and discontinuous feedback signals thus making it a hybrid feedback control system. The control law used in the SMC is based on the current as well as the future state of the system, thus providing a feedback loop which helps the system to slide along the desired surface, i.e. the system moves in the desired trajectory.

Moreover, it offers various advantages over the traditional PID controller, like easier implementation, no drift in controller output with time and a faster response time, easy to model non-linear systems.

For our system, which is described as,

$$\dot{x}(t) = Ax(t) + Bu(t) + \delta f(t) \quad (6.3)$$

where,  $f(t) =$  Disturbance,

Sliding Surface or the desired system behavior has been described as

$$\sigma = s^T \tilde{x} \quad (6.4)$$

where,  $s^T =$  Sliding surface parameter and  $\tilde{x} = x - x_d =$  State Error  
 $x =$  Current state of the AUV,  $x_d =$  Next set waypoint of the AUV.

It is important that the SMC is designed in such a way that the sliding surface, i.e. the state error tends to zero. The sliding surface reaches zero in a finite amount of time under the condition,

$$\dot{\sigma} = -\eta sgn(\sigma) \quad (6.5)$$

where,  $\eta =$  switching gain of the controller.

From the eqns 4.4 and 4.5,

$$s^T \dot{\tilde{x}} = -\eta sgn(\sigma) s^T (Ax + Bu + \delta f - \dot{x}_d) = -\eta sgn(\sigma) \quad (6.6)$$

Solving equation 4.6, we get the following control law,

$$u = -(s^T b)^{-1} s^T Ax + (s^T b)^{-1} [-s^T \delta f + s^T \dot{x}_d - \eta sgn(\sigma)] \quad (6.7)$$

If (A,b) is controllable and  $(s^T b)$  is non zero, then it may be shown that the sliding mode coefficients,  $s^T$ , are the elements of the left eigen vector of the closed loop dynamics matrix  $(A - bk)$  corresponding to the pole at zero, where  $k$  is the

feedback gain matrix of the state space system.  $k$  can be obtained from the pole placement method for the desired closed loop poles of the system such that,

$$s^T[A - bk] = 0 \quad (6.8)$$

Since,  $sgn()$  is a hard limiting function which is impossible to implement in real world system, we use the tanh function to derive the final control law given by

$$u = -kx - (s^T b)^{-1} s^T \delta f - (s^T b)^{-1} s^T \dot{x}_d - \eta (s^T b)^{-1} \tanh\left(\frac{\sigma}{\phi}\right) \quad (6.9)$$

where,  $\phi$  = Boundary layer thickness of sliding surface. i.e. tolerance. It acts like a low pass filter to remove chattering.

## 6.3 Control Law derivation

In this section we describe the derivation of the control law for both the Depth plane control and Heading Plane control.

### 6.3.1 Depth Plane Control

The state space system describing the Depth plane system is,

$$\begin{bmatrix} \dot{q} \\ \dot{\theta} \\ \dot{Z} \end{bmatrix} = \begin{bmatrix} -1.5005 & -0.9669 & 0 \\ 1 & 0 & 0 \\ 0 & -1.25 & 0 \end{bmatrix} \begin{bmatrix} q \\ \theta \\ Z \end{bmatrix} + \begin{bmatrix} -4.3994 \\ 0 \\ 0 \end{bmatrix} \delta_s \quad (6.10)$$

Taking following points into consideration,

- We have to make the Depth plane system including the controller, as a Type-1 system, so that AUV can follow both step input as well as ramp input, which are the general inputs to any path tracking AUV.
- Let us consider a Maximum Overshoot of less than 3%,
- Let us consider a settling time of less than 4 secs and

The desirable closed loop poles for the system is,  $ClosedLoopPoles = [0, -0.41, -0.45]$

Thus the feedback gain system for the above mentioned closed loop poles are,  $K = [0.1456, 0.1778, 0]$

Therefore, the sliding surface coefficients of the system are,  $s^T = [6.7751, 5.8266, -1]$  and  $s^T b = -29.8062$ .

Hence, the control law for the Depth Plane Control is,

$$\begin{aligned} \delta_s &= -0.145q - 0.1778\theta + 2.4 \tanh\left(\frac{\sigma}{4}\right) \\ \sigma &= 6.7751\tilde{q} + 5.8266\tilde{\theta} - \tilde{Z} \end{aligned} \quad (6.11)$$

Thus, using the above mentioned control law we can implement the SMC in the Depth plane Motion of the AUV.

The Response of the system to various trajectories are given below,

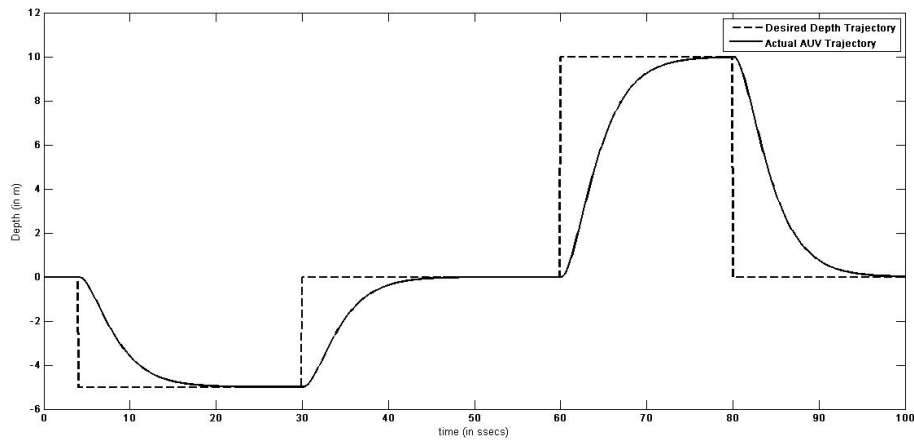


Figure 6.5: System Response to Step Input Trajectory (Depth vs Time)

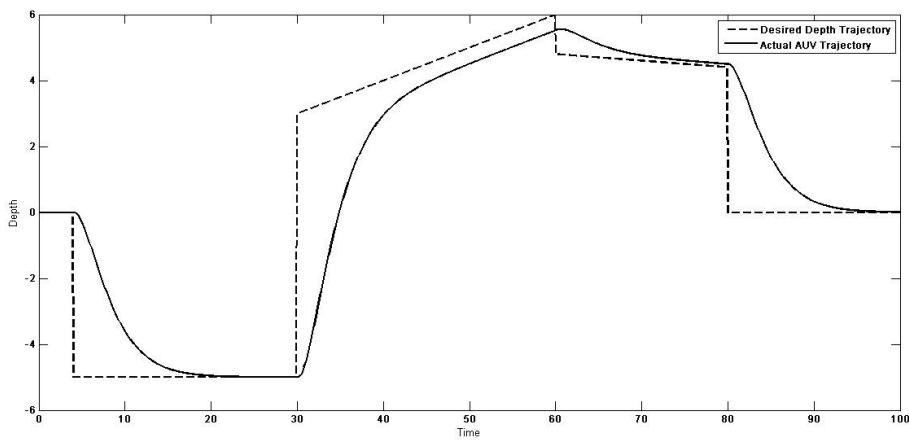


Figure 6.6: System Response to ramp input trajectory (Depth vs. Time)

From the above system response graphs, we observe that the controller enables the AUV to follow the trajectory with step changes with zero steady state error, but with ramp changes finite steady state error exists. However, the steady state error is within acceptable limits and the system is able to track the desired trajectory. Therefore, with the addition of SMC, depth plane system becomes stable and is able to track the trajectory.

### 6.3.2 Heading Plane Control

The state space system describing the Heading plane system is,

$$\begin{bmatrix} \dot{v} \\ \dot{r} \\ \dot{\psi} \end{bmatrix} = \begin{bmatrix} -0.6782 & -0.3261 & 0 \\ -5.0571 & -1.3002 & 0 \\ 0 & 1 & 0 \end{bmatrix} \begin{bmatrix} v \\ r \\ \psi \end{bmatrix} + \begin{bmatrix} 1.2103 \\ -5.1563 \\ 0 \end{bmatrix} \delta_s \quad (6.12)$$

Taking following points into consideration,

- We have to make the Depth plane system including the controller, as a Type-1 system, so that AUV can follow both step input as well as ramp input, which are the general inputs to any path tracking AUV.
- Let us consider a Maximum Overshoot of less than 2.5%,
- Let us consider a settling time of less than 5 secs and

The desirable closed loop poles for the system is,  $ClosedLoopPoles = [0, -0.67, -0.73]$

Thus the feedback gain system for the above mentioned closed loop poles are,  $K = [2.3046, 0.6616, 0]$

Therefore, the sliding surface coefficients of the system are,  $s^T = [-0.8924, -0.4469, -0.0623]$  and  $s^T b = 1.2241$ .

Hence, the control law for the Heading Plane Control is,

$$\begin{aligned} \delta_r &= -2.3406v - 0.6616r - 1.6 \tanh\left(\frac{\sigma}{0.07}\right) \\ \sigma &= -0.8924\tilde{v} - 0.4469\tilde{r} - 0.0623\tilde{\psi} \end{aligned} \quad (6.13)$$

Thus, using the above mentioned control law we can implement the SMC in the Heading plane Motion of the AUV. The Response of the system to various trajectories are given below,

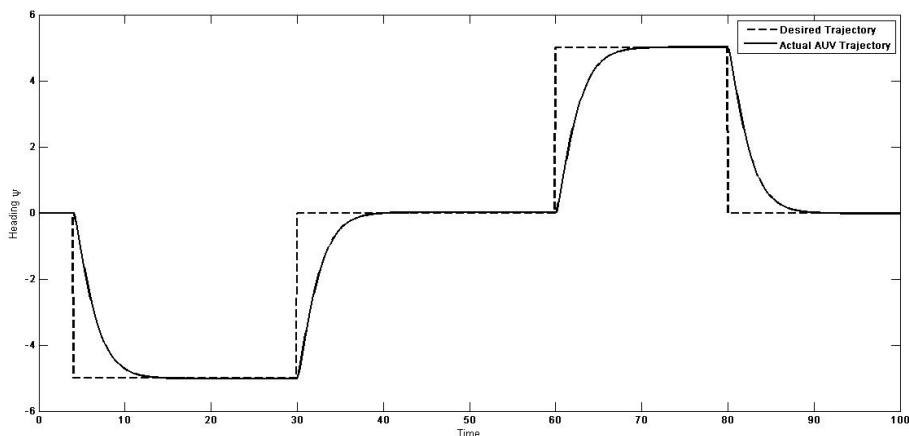


Figure 6.7: System Response to Step Input Trajectory (Heading( $\psi$ ) vs Time

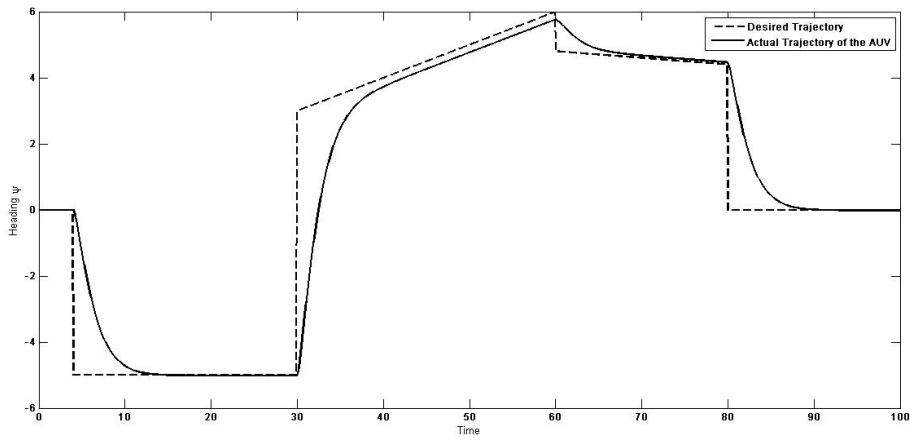


Figure 6.8: System Response to ramp input trajectory (Heading( $\psi$ ) vs. Time)

From the above system response graphs, we observe that the controller enables the AUV to follow the trajectory with step changes with zero steady state error, but with ramp changes finite steady state error exists. However, the steady state error is within acceptable limits and the system is able to track the desired trajectory. Therefore, with the addition of SMC, heading plane system becomes stable and is able to track the desired trajectory.



# Chapter 7

## Conclusion

Through this project we have tried to demonstrate a low cost method of determining AUV model using Computational Fluid Dynamics and empirical formulae. The process described was applied to the prototype AUV and a mathematical model was presented for analysis using computer simulations. This mathematical model was then used to design Sliding Mode controller to implement path following task. Results obtained were found to be satisfactory and in tandem with the theoretical premise. From the response of the system it was observed that the system was able to track step changes in trajectory with zero steady state errors, while it showed finite steady state error when tracking ramp type changes in trajectory. Although the error was within acceptable limits. Therefore we can conclude that the designed controller was successful in tracking the desired path.

In chapter -2, we derived the physical parameters of the already built prototype AUV, by creating a CAD model of the real world AUV. We, also found out the drag parameter of the AUV using CFD. These parameters were of utmost importance in finding out the AUV coefficients as well as in mathematical modelling of the system.

In chapter 3 we derived the AUV hydrodynamic coefficients using empirical formula and AUV data. These, coefficients represent an important analysis of how the AUV behaves under water. In chapter 4, AUV modelling and simulation results were shown, using rudder and stern angle as input to the system. This simulation helps us to estimate how the system behaves under the absence of the controller. We linearised and decoupled the entire AUV model into two parts the Depth Plane Motion and the Heading Plane Motion in chapter 5 and also adjusted the parameter formulas for operation of AUV around a fixed operating point with small perturbations. Thus, finally we derived the state space model of the Depth Plane as well as Heading Plane motion of the AUV.

Finally, in chapter-6, we analysed the decoupled system and found that the Depth Plane model was stable as well as controllable but the system response was sluggish and not upto the desired standard. Whereas, the Heading Plane System was unstable but controllable and the system response was diverging. Thus, a need for controller was felt. For this purpose Sliding Mode Controller was proposed because it solves dual purpose, one is to keep the system in desired state and second since the control law uses present as well as future state of system to determine the control signal, it can be easily incorporated to be included for the Path Following algorithm. Using, Pole placement method, desired closed loop poles were incor-

porated into the system and feedback gain was calculated. After which sliding surface coefficients were found out and control law established. From the response of both the system, it can be observed that Depth Plane Model as well as Heading Plane Model becomes stable as well as follows the trajectories accurately, when the design Sliding Mode controller is included in each of the system.

## 7.1 Scope for Future Research

Future research in the field includes the topics as given below,

- Field Testing of AUV and Verification of the Mathematical Model described in the thesis
- Inclusion of Wave disturbances in the design of controller. Since, we have chosen Sliding Mode Controller, it becomes relatively easier to include wave disturbances in the control system.
- Modelling of the AUV system in shallow waters
- Improvement in the methodology applied for Derivation of coefficients to include the effects of wave and other oceanic disturbances
- Waypoint Selection Method

# Appendix

## Appendix A - AUV Parameters

Parameters	Value	Parameters	Value
Xuu	-1.36 kg/m	Kpdot	-0.0416 kg-m <sup>2</sup> /rad
Yvv	-90.9473 kg/m	Kqdot	0
Yrrd	0.9930 kg-m/rad <sup>2</sup>	Krdot	0
Zww	-90.9473 kg/m	Mudot	0
Zqqd	- 0.9930 kg-m/rad <sup>2</sup>	Mvdot	0
Mwwd	2.0298 kg	Mwdot	2.2586 kg-m
Mqq	0.4173 kg-m <sup>2</sup> /rad <sup>2</sup>	Mpdot	0
Nvvd	- 2.0298 kg	Mqdot	-2.3441 kg-m <sup>2</sup> /rad
Nrr	0.4173 kg-m <sup>2</sup> /rad <sup>2</sup>	Mrdot	0
Kpp	-0.085 kg-m <sup>2</sup> /rad	Nudot	0
Yuv	-14.75 kg/m	Nvdot	-2.2586 kg-m
Zuw	-14.75 kg/m	Nwdot	0
Muwb	-2.62 kg	Npdot	0
Nuvb	2.62 kg	Nqdot	0
Xudot	-0.57858 kg	Nrdot	-2.3441 kg-m <sup>2</sup> /rad
Xvdot	0	Xuq	0
Xwdot	0	Xwq	-24.0189 kg/rad
Xpdot	0	Xqq	2.2586 kg-m/rad
Xqdot	0	Xvr	24.0189 kg/rad
Xrdot	0	Xrp	0
Yudot	0	Xrr	2.2586 kg-m/rad
Yvdot	-24.0189 kg	Xur	0
Ywdot	0	Xwr	0
Ypdot	0	Xvq	0
Yqdot	0	Xpq	0
Yrdot	-2.2586 kg-m/rad	Xqr	0
Zudot	0	Yvr	0
Zvdot	0	Yvp	0
Zwdot	-24.0189 kg	Yrra	0
		Yrp	0
		Ypp	0
		Yup	0

Parameters	Value	Parameters	Value
Zpdot	0	Ywr	0
Zqdot	2.2586 kg-m/rad	Yura	-0.57858 kg/rad
Zrdot	0	Ywp	24.0189 kg/rad
Kudot	0	Ypq	- 2.2586 kg-m/rad
Kvdot	0	Yqr	0
Kwdot	0	Zwq	0
Zuqa	0.57858 kg/rad	Mwp	0
Zqqa	0	Mur	0
Zvp	-24.0189 kg/rad	Mpq	0
Zrp	-2.2586 kg/rad	Mqr	0
Zpp	0	Nuu	0
Zup	0	Nwu	0
Zwp	0	Nuq	0
Zvq	0	Nwq	0
Zpq	0	Nqq	0
Zqr	0	Nvva	0
		Nvr	0
Kwu	0	Nvp	0
Kuq	0	Nrp	0
Kww	0	Npp	0
Kwq	0	Nuva	-23.44 kg
Kqq	0	Nvw	0
Kvv	0	Nup	0
Kvr	0	Nura	-2.2586 kg-m/rad
Kvp	0	Nwp	2.2586 kg-m/rad
Krr	0	Nvq	0
Krp	0	Npq	-2.3025 kgm <sup>2</sup> /rad <sup>2</sup>
Kuv	0	Nqr	0
Kvw	0		
Kwr	0	Xprop	2.04 N
Kwp	0	Kprop	-0.3248 Nm
Kur	0		
Kvq	0	Yuudr	24.94 kg/(m-rad)
Kpq	0	Zuuds	-24.94 kg/(m-rad)
Kqr	0	Muuds	-10.17 kg/rad
		Nuudr	-10.17 kg/rad
Mwq	0	Yuvf	-24.94 kg/m
Muqa	-2.2586 kg-m/rad	Zuuf	-24.94 kg/m
Muu	0	Yurf	10.17 kg/rad
Mwwa	0	Zuqf	-10.17 kg/rad
Muwa	23.44 kg	Muwf	-10.17 kg
Mvr	0	Nuvf	10.17 kg
Mvp	2.3025 kg-m/rad	Muqf	-4.1473 kg-m/rad
Mpp	0	Nurf	-4.1473 kg-m/rad
Mrr	0	Mvw	0
Mrp	2.3025 kgm <sup>2</sup> /rad <sup>2</sup>	Mup	0
Muv	0	Mwr	0

# Appendix B - Matlab Codes

## Matlab Code for AUV Simulation

```
function output_table = auv_sim(delta_s,delta_r)
%EXPERIMENTAL/ASSIGNED VALUES: intial conditions, input vector

% loading model inputs, generated in SIM_SETUP.M

for i = 1:1:10001
    ui(1,i) = delta_s;
    ui(2,i) = delta_r;

end
time_step = 0.1;
x = [0;0;0;0;0;0;0;0;0;0;0;0;0;0];

pitch_max=90;

%RUN MODEL

n_steps=size(ui,2)-1;
output_table=zeros(n_steps,size(x,1)+size(ui,1)+7);

%MAIN PROGRAM
for i=1:n_steps
%Store current states x(n), input ui(n) and time in seconds
output_table(i,1:14)=[x' ui(:,i)'];
output_table(i,21)=(i-1)*time_step;

%Calculate forces and accelerations
%
%CALL AUV.M
%
%xdot(i)=f(x(i),u(i));
[xdot,forces]=auv(x,ui(:,i)');

%Store forces at step n
output_table(i,15:20) = forces';

%IMPROVED RUNGE_KUTTA APPROXIMATION to calculate new states
%NOTE:ideally,should be approximating ui values for k2,k3
%i.e. ((ui(:,i)+ui(:,(i+1))))/2
k1_vec=xdot;
k2_vec=auv(x+(0.5.*time_step.*k1_vec),((ui(:,i)+ui(:,i+1))./2)');
k3_vec=auv(x+(0.5.*time_step.*k2_vec),((ui(:,i)+ui(:,i+1))./2)');
k4_vec=auv(x+(time_step.*k3_vec),ui(:,i+1)');
x=x+time_step/6.*(k1_vec+2.*k2_vec+2.*k3_vec+k4_vec);
```

```

end
end

%function to return time derivative of state variables
function [accelerations,forces] = auv(x,ui)

% x = [u v w p q r xpos ypos zpos phi theta psi]'
% Body Referenced coordinates
% u = Surge Velocity
% v = Sway Velocity
% w = Heave Velocity
% p = roll rate
% q = pitch rate
% r = yaw rate
% Earth Fixed coordinate
% xpos
% ypos
% zpos
% phi = roll angle
% theta = pitch angle
% psi = yaw angle
%
% Input Vector
% ui = [delta_s delta_r]'
% Control fin angles
%
%%
%Initialise global Variables for own
Xuu = -1.36;
Xwq = -24.0189;
Xqq = 2.2586;%-2.2586;
Xvr = 24.0189;
Xrr = 2.2586;%-2.2586;
Xprop = 2.04;
Yvv =-90.947;
Yrr = 0.9930;
Yuv = -39.69;
Ywp = 24.0189;
Yur = 9.59142;
Ypq = -2.2586;%2.2586;
Yuudr = 24.94;
Zww =-90.9473;
Zqq = -0.993;
Zuw = -39.69;
Zuq = -9.59;
Zvp = -24.0189;
Zrp = -2.2586;%2.2586;
Zuuds = -24.94;

```

```

Kpp = -0.085;
Kprop = -0.3248;
Mww = 2.0298;
Mqq = - 0.4173;%0.4173
Muq = -6.4059;%-1.8887;%-6.4059;
Muw = 10.65;
Mvp = 2.2586;%-2.2586;
Muuds = -10.17;
Mrp = 2.3025;
Nvv = -2.0298;
Nrr = -0.4173;
Nuv = -10.65;
Npq = -2.3025;
Nwp = 2.2586;%-2.2586;
Nur = -6.4059;%-1.8887;%-6.4059;
Nuudr = -10.17;

xg = 0;
yg = 0;
zg = 0.02;
xb = 0;%-0.5191;
yb = 0;
zb = 0;
W = 174.618;
m = 17.8;
B =176.58;
% buoyancy = 18;

Xudot = -0.57858;
Yvdot = -24.0189;
Yrdot = -2.2586;%2.2586;
Zwdot = -24.0189;
Zqdot = 2.2586;%-2.2586;
Ixx = 0.053437682;
Kpdot = -0.0416;
Mwdot = 2.2586;%-2.2586;
Mqdot = -2.3441;
Iyy = 1.267861759;
Nvdot = -2.2586;%2.2586 ;
Nrdot = -2.3441;
Izz = 1.267861759;

mass_mat = [(m-Xudot),0,0,0,m*zg,-m*yg;
0,(m-Yvdot),0,-m*zg,0,(m*xg - Yrdot);
0,0,(m-Zwdot),m*yg,(-m*xg-Zqdot),0;
0,-m*zg,m*yg,(Ixx-Kpdot),0,0;
m*zg,0,(-m*xg-Mwdot),0,(Iyy-Mqdot),0;
-m*yg,(m*xg-Nvdot),0,0,0,(Izz-Nrdot)];

```

```

Minv = inv(mass_mat);
% output flags

delta_max = pi/4;
% get state variables
u = x(1) ;v = x(2) ;w = x(3) ;p = x(4) ;q = x(5) ;
r = x(6) ;phi = x(10) ;theta = x(11) ;psi = x(12) ;

% get control Inputs
delta_s = ui(1); delta_r = ui(2);

% Check Control Inputs
if delta_s > delta_max
    delta_s = sign(delta_s)*delta_max;
end
if delta_r > delta_max
    delta_r = sign(delta_r)*delta_max;
end

% Initialise elements of coordinate system transform matrix
c1 = cos(phi); c2 = cos(theta); c3 = cos(psi); s1 = (sin(phi));
s2 = sin(theta); s3 = sin(psi);t2 = tan(theta);

% Set total forces from equations of motion
X = -(W-B)*sin(theta) + Xu*u*abs(u)+(Xwq-m)*w*q+(Xqq+ m*xg)*q^2 ...
    +(Xvr+m)*v*r + (Xrr + m*xg)*r^2 - m*yg*p*q - m*zg*p*r + Xprop;

Y = (W-B)*cos(theta)*sin(phi) + Yvv*v*abs(v) + (Yrr*r*abs(r)) + Yuv*u*v ...
    + (Ywp +m)*w*p + (Yur - m)*u*r - (m*zg)*q*r + (Ypq - m*xg)*p*q ...
    + Yuudr*u^2*delta_r;

Z = (W-B)*cos(theta)*cos(phi) + Zww*w*abs(w) + Zqq*q*abs(q) + Zuw*u*w ...
    + (Zuq+m)*u*q + (Zvp - m)*v*p + (m*zg)*p^2 + (m*zg)*q^2 ...
    + (Zrp - m*xg)*r*p + Zuuds*u^2*delta_s;

K = -(yg*W-yb*B)*cos(theta)*cos(phi) - (zg*W-zb*B)*cos(theta)*sin(phi) ...
    +Kpp*p*abs(p) - (Izz-Iyy)*q*r - (m*zg)*w*p + (m*zg)*u*r + Kprop;

M = -(zg*W-zb*B)*sin(theta) - (xg*W - xb*B)*cos(theta)*cos(phi) + Mww*w*abs(w) ...
    + Mqq*q*abs(q) + (Mrp - (Ixx-Izz))*r*p + (m*zg)*v*r - (m*zg*w*q) ...
    +(Muq - m*xg)*u*q + Muw*u*w + (Mvp + m*xg)*v*p + Muuds*u^2*delta_s;

N = (-xg*W-xb*B)*cos(theta)*sin(phi) - (yg*W-yb*B)*sin(theta) + Nvv*v*abs(v) ...
    + Nrr*r*abs(r) + Nuv*u*v + (Npq -(Iyy-Ixx))*p*q + (Nwp - m*xg)*w*p ...
    +(Nur + m*xg)*u*r + Nuudr*u^2*delta_r;

forces = [X Y Z K M N]';

```



```

accelerations = ...
    [Minv(1,1)*X+Minv(1,2)*Y+Minv(1,3)*Z+Minv(1,4)*K+Minv(1,5)*M+Minv(1,6)*N
    Minv(2,1)*X+Minv(2,2)*Y+Minv(2,3)*Z+Minv(2,4)*K+Minv(2,5)*M+Minv(2,6)*N
    Minv(3,1)*X+Minv(3,2)*Y+Minv(3,3)*Z+Minv(3,4)*K+Minv(3,5)*M+Minv(3,6)*N
    Minv(4,1)*X+Minv(4,2)*Y+Minv(4,3)*Z+Minv(4,4)*K+Minv(4,5)*M+Minv(4,6)*N
    Minv(5,1)*X+Minv(5,2)*Y+Minv(5,3)*Z+Minv(5,4)*K+Minv(5,5)*M+Minv(5,6)*N
    Minv(6,1)*X+Minv(6,2)*Y+Minv(6,3)*Z+Minv(6,4)*K+Minv(6,5)*M+Minv(6,6)*N
    c3*c2*u + (c3*s2*s1-s3*c1)*v + (s3*s1*c3*c1*s2)*w
    s3*c2*u + (c1*c3*s1*s2*s3)*v + (c1*s2*s3-c3*s1)*w
    -s2*u +                c2*s1*v +                c1*c2*w
    p +                s1*t2*q +                c1*t2*r
                c1*q -                s1*r
                s1/c2*q +                c1/c2*r ];

end

```

## Matlab Code to Calculate Hydrodynamic Coefficients

```

% To calculate the Added Mass coefficients of the AUV
load('R_Rev.mat');
load('X_Rev.mat');
R = R_rev/100;
X = X_rev/100;
afin = 0.1673; %Own AUV
% % afin = 0.13; %REMUS AUV
k = pi*1030;
k1 = k*afin*afin;
k2 = k/(afin*afin);
%Own AUV
X1 = X(1:19);
X2 = X(19:41);
X3 = X(41:155);
R1 = R(1:19);
R2 = R(19:41);
R3 = R(41:155);
x2diff=X(41)-X(19);

Yvdot=(-k*trapz(X1,R1.*R1))+(-k1*x2diff)+(k*trapz(X2,R2.*R2))-
(k2*trapz(X2,R2.*R2.*R2.*R2))+(-k*trapz(X3,R3.*R3))
Mwdot=(-k*trapz(X1,X1.*R1.*R1))+(-k1*trapz(X2,X2))+ (k*trapz(X2,X2.*R2.*R2))-
(k2*trapz(X2,X2.*R2.*R2.*R2.*R2))+(-k*trapz(X3,X3.*R3.*R3))
Mqdot=(-k*trapz(X1,X1.*X1.*R1.*R1))+(-k1*trapz(X2,X2.*X2))+
(k*trapz(X2,X2.*X2.*R2.*R2))- (k2*trapz(X2,X2.*X2.*R2.*R2.*R2.*R2))
+(-k*trapz(X3,X3.*X3.*R3.*R3))

% Program to calculate the cross-flow drag Coefficients
load('R_rev.mat');
load('X_rev.mat');
k = 0.5*1030*0.607*0.008645;

```

```

k1 = 0.5*1030*1.1;
R1 = R_rev/100;
X1 = X_rev/100;
X1

Yvv = ((-k1)*trapz(X1,(2.*R1)))-(2*k)
Mww = (k1*trapz(X1,(2.*X1.*R1)))+(2*k*0.4078)
Yrr = (-k1*trapz(X1,(2.*X1.*abs(X1).*R1)))+(2*k*0.4078*0.4078)
Nrr = (k1*trapz(X1,(2.*X1.*X1.*X1.*R1)))-(2*k*0.4078*0.4078*0.4078)

```

## Depth Plane Controller Design

```

clc
clear all
close all
% Ideal Path
t = 0:0.1:100;
for i = 1:1:1001
    if(t(i)<4)
        zd(i) = 0;
    elseif 4<=t(i)&&t(i)<30
        zd(i) = -5;
    elseif 30<=t(i)&&t(i)<60
        zd(i) = 0.1*t(i);
    elseif 60<=t(i)&&t(i)<80
        zd(i) = 6-0.02*t(i);
    else
        zd(i) = 0;
    end
end

%% Depth Control Law

%X = [q,theta,z], u = [delta_s]
M3 = [3.612,0,0;
      0,0,1;
      0,1,0];
Cd3 = [-5.41982,-3.49236,0;
       0,-1.25,0;
       1,0,0];
D3 = [-15.890625;0;0];

% X_dot = AX + Bu

A3 = inv(M3)*Cd3;
B3 = inv(M3)*D3;

```

```

U3=[B3,A3*B3,A3*A3*B3]
Rank3=rank(U3)
poles = eig(A3)
sys = ss(A3,B3,[0 0 1],0);
figure
rlocusplot(sys)
figure
bode(sys)
% A3
% B3
% U3
% Rank3
%% Let closed loop poles be at [0,-0.25,-0.26];
J = [0,-0.45,-0.41];

% K = feedback gain matrix.
K = place(A3,B3,J)
[V,D] = eig(transpose(A3)-transpose(B3*K));
% Sliding Surface parameter = S_t
S_t = transpose(V(:,3));
aa = min(abs(S_t));
S_t = S_t/(-aa)
(S_t*B3)
sys = ss(A3-B3*K,B3,[0 0 1],0);
figure
rlocusplot(sys)
figure
bode(sys)

%% EXPERIMENTAL/ASSIGNED VALUES: intial conditions, input vector

% loading model inputs, generated in SIM_SETUP.M

time_step = 0.1;
x = [0;0;0]; % x = [q,theta,z];
xdot = [0;0;0];
pitch_max=90;

%RUN MODEL
for i=1:1:1001
    [delta_s,s] = stern_angle( K,x,S_t,zd(i) );
    %Store current states x(n), input ui(n) and time in seconds
    op(i,:) = [x',delta_s,s];

    xdot=auv_exp(x,delta_s,A3,B3);
    %xdot(3)
    %IMPROVED EULER INTEGRATION to calculate new states

```

```

k1_vec=x+(xdot.*time_step);
[delta_s,s] = stern_angle( K,k1_vec,S_t,zd(i) );
k2_vec=auv_exp(k1_vec,delta_s,A3,B3);
x=x+0.5.*time_step.*(xdot+k2_vec);

end

figure
plot(t,zd,t,op(:,3));
figure
plot(t,op(:,4));

function [delta_s,sigma] = stern_angle( K,x,S_t,zd )
% Program To calculate the Stern angle Input
qtilde = x(1) - 0;
thetatile = x(2)-0;
ztilde = x(3)-zd;
sigma = (S_t(1)*qtilde) + (S_t(2)*thetatile) + (S_t(3)*ztilde);
delta_s = (-K(1)*x(1))-K(2)*x(2))+
(2.4*tanh(((S_t(1)*qtilde) + (S_t(2)*thetatile) + (S_t(3)*ztilde))/4));

end

%function to return time derivative of state variables
function xdot = auv_exp(x,u,A,B)
xdot = A*x + B*u;
end

```

## Heading Plane Controller Design

```

clc
clear all
close all
% Ideal Path
t = 0:0.1:100;
for i = 1:1:1001
    if(t(i)<4)
        zd(i) = 0;
    elseif 4<=t(i)&&t(i)<30
        zd(i) = -5;
    elseif 30<=t(i)&&t(i)<60
        zd(i) = 0;
    elseif 60<=t(i)&&t(i)<80
        zd(i) = 5;
    else
        zd(i) = 0;
    end
end

```

```

end

%% Depth Control Law

% X = [v,r,,psi], u = [delta_r]

M3 = [41.8189,2.2586,0;
      2.2586,3.61196,0;
      0,0,1];

Cd3 = [-39.78196,-16.575269,0;
      -19.7976,-5.43284,0;
      0,1,0];
D3 = [38.96875;-15.890625;0];

% X_dot = AX + Bu

A3 = inv(M3)*Cd3;
B3 = inv(M3)*D3;
eig(A3);
sys = ss(A3,B3,[0 0 1],0);
% figure
% rlocusplot(sys)
% figure
% bode(sys)
%% Let closed loop poles be at [0,-0.73,-0.67];
J = [0,-0.73,-0.67];

% K = feedback gain matrix.
K = place(A3,B3,J)
[V,D] = eig(transpose(A3)-transpose(B3*K));
% Sliding Surface parameter = S_t
S_t = transpose(V(:,3));
aa = min(abs(S_t));
S_t = S_t/(-1)
S_t*B3
sys = ss(A3-B3*K,B3,[0 0 1],0);
figure
rlocusplot(sys)
figure
bode(sys)

%% EXPERIMENTAL/ASSIGNED VALUES: intial conditions, input vector

% loading model inputs, generated in SIM_SETUP.M

```

```

time_step = 0.1;
x = [0;0;0]; % x = [q,theta,z];
xdot = [0;0;0];
pitch_max=90;

%RUN MODEL
for i=1:1:1001
    delta_r = rudder_angle( K,x,S_t,zd(i) );
    %Store current states x(n), input ui(n) and time in seconds
    op(i,:) = [x',delta_r];

    xdot=auv_exp(x,delta_r,A3,B3);
    %xdot(3)
    %IMPROVED EULER INTEGRATION to calculate new states

    k1_vec=x+(xdot.*time_step);
    delta_r = rudder_angle( K,k1_vec,S_t,zd(i) );
    k2_vec=auv_exp(k1_vec,delta_r,A3,B3);
    x=x+0.5.*time_step.*(xdot+k2_vec);

end
figure
% plot(t,op(:,1));
% figure
% plot(t,op(:,2));
% figure
plot(t,zd,t,op(:,3));
figure
plot(t,op(:,4));

function delta_s = rudder_angle( K,x,S_t,zd )
% Function to calculate Rudder Angle Input
qtilde = x(1) - 0;
thetatilde = x(2)-0;
ztilde = x(3)-zd;
delta_s = (-K(1)*x(1))-(K(2)*x(2))+
(-1.6*tanh(((S_t(1)*qtilde) + (S_t(2)*thetatilde) + (S_t(3)*ztilde))/0.07));

end

%function to return time derivative of state variables
function xdot = auv_exp(x,u,A,B)
xdot = A*x + B*u;
end

```

# References

1. Martin Abkowitz. Stability and Motion Control of Ocean AUVs. MIT Press, Cambridge, MA, 1972.
2. B. Allen, R. Stokey, T. Austin, N. Forrester, R. Goldsborough, M. Purcell, and C. von Alt. REMUS: A small, low cost AUV; system description, field trials and performance results. In Proceedings MTS/IEEE Oceans 1997, Halifax, Canada, 1997. 37
3. B. Allen, W. Vorus, and T. Prestero. Propulsion system performance enhancements on REMUS AUVs. In Proceedings MTS/IEEE Oceans 2000, Providence, Rhode Island, September 2000.
4. P. Edgar An. An experimental self-motion study of the Ocean Explorer AUV in controlled sea states. IEEE Journal of Oceanic Engineering, 23(3):274-284, 1998.
5. P. Ananthkrishnan. Dynamic response of an underwater body to surface waves. In Proceedings ASME Forum on Advances in Free Surface and Interface Fluid Dyanamics, San Francisco, CA,1999.
6. Robert D. Blevins. Formulas for Natural Frequency and Mode Shape. Kreiger Publishing,Florida, 1979. 28, 29
7. M. R. Bottaccini. The stability coefficients of standard torpedoes. NAVORD Report 3346, U.S.Naval Ordnance Test Station, China Lake, CA, 1954.
8. J. Feldman. Revised standard submarine equations of motion. Report DTNSRDC/SPD-0393-09, David W. Taylor Naval Ship Research and Development Center, Bethesda, MD, June 1979.
9. John E. Fidler and Charles A. Smith. Methods for predicting submersible hydrodynamic characteristics.Report NCSC TM-238-78, Naval Coastal Systems Laboratory, Panama City, FL,1978.
10. Thor 1. Fossen. Guidance and Control of Ocean Vehicles. John Wiley Sons, New York, 1994.
11. R. W. Fox and A. T. McDonald. Introduction to Fluid Mechanics. J. Wiley and Sons, New York, 4th edition, 1992.
12. M. Gertler and G. Hagen. Standard equations of motion for submarine simulation. Report DTNSRDC 2510, David W. Taylor Naval Ship Research and Development Center, Bethesda,MD, June 1967.

13. Michael J. Griffin. Numerical prediction of the forces and moments on submerged bodies operating near the free surface. In Proceedings of the 2000 SNAME/ASNE Student Paper Night, Massachusetts Institute of Technology, January 2000. SNAM
14. Michael F. Hajosy. Six Degree of Freedom Vehicle Controller Design for the Operation of an Unmanned Underwater Vehicle in a Shallow Water Environment. Ocean Engineer's thesis, Massachusetts Institute of Technology, Department of Ocean Engineering, May 1994.
15. Sighard F. Hoerner. Fluid Dynamic Drag. Published by author, 1965.
16. Sighard F. Hoerner and Henry V. Borst. Fluid Dynamic Lift. Published by author, second edition, 1985.
17. P. C. Hughes. Spacecraft Attitude Dynamics. John Wiley and Sons, New York, 1986.
18. D. E. Humphreys. Development of the equations of motion and transfer functions for underwater vehicles. Report NCSL 87-76, Naval Coastal Systems Laboratory, Panama City, FL, July 1976.
19. D. E. Humphreys. Dynamics and hydrodynamics of ocean vehicles. In Proceedings MTSj1EEE Oceans 2000, Providence, Rhode Island, September 2000.
20. E. V. Lewis, editor. Principles of Naval Architecture. Society of Naval Architects and Marine Engineers, Jersey City, New Jersey, second edition, 1988.
21. Woei-Min Lin and Dick Y. P. K. Yue. Numerical solutions for large-amplitude ship motions in the time domain. In Proceedings Eighteenth Symposium on Naval Hydrodynamics, Ann Arbor, Michigan, 1990.
22. D. F. Myring. A theoretical study of body drag in subcritical axisymmetric flow. Aeronautical Quarterly, 27(3):186-94, August 1976.
23. Meyer Nahon. A simplified dynamics model for autonomous underwater vehicles. In Proceedings 1996 Symposium on Autonomous Underwater Vehicle Technology, pages 373-379, June 1996.
24. J. N. Newman. Marine Hydrodynamics. MIT Press, Massachusetts, 1977.
25. Norman S. Nise. Control Systems Engineering. Benjamin/Cummings, San Francisco, CA, first edition, 1992.



# Bibliography

1. William D. Ramsey. Boundary Integral Methods for Lifting Bodies with Vortex Wakes. PhD dissertation, Massachusetts Institute of Technology, Department of Ocean Engineering, May 1996.
2. Jeffery S. Riedel. Seaway Learning and Motion Compensation in Shallow Waters for Small AUVs. PhD dissertation, Naval Postgraduate School, Department of Ocean Engineering, June 1999.
3. R. Stokey and T. Austin. Sequential long baseline navigation for REMUS, an autonomous underwater vehicle. In Proceedings Information Systems for Navy Divers and AUVs Operating in Very Shallow Water and Surf Zone Regions, April 1999.
4. Michael S. Triantafyllou. Maneuvering and control of surface and underwater vehicles. Lecture Notes for MIT Ocean Engineering Course 13.49, 1996.
5. C. von Alt, B. Allen, T. Austin, and R. Stokey. Remote environmental monitoring units. In Proceedings MTS/IEEE Oceans 1994, Cambridge, MA, 1994.
6. C. von Alt and J.F. Grassle. LEO-15: An unmanned long term environmental observatory. In Proceedings MTS/IEEE Oceans 1992, Newport, RI, 1992.
7. L. F. Whicker and L. F. Fehlner. Free-stream characteristics of a family of low-aspect ratio control surfaces. Technical Report 933, David Taylor Model Basin, 1958. NC.
8. Christopher J. Wily. Attitude Control of an Underwater Vehicle Subjected to Waves. Ocean Engineer's thesis, Massachusetts Institute of Technology, Department of Ocean Engineering, May 1994.
9. Ming Xue. Three-dimensional fully non-linear simulation of waves and wave-body interactions. PhD dissertation, Massachusetts Institute of Technology, Department of Ocean Engineering, May 1997.
10. D. R. Yoerger, J.G. Cooke, and J.-J. E. Slotine. The influence of thruster dynamics on underwater vehicle behavior and their incorporation into control system design. IEEE Journal of Oceanic Engineering, 15:167-178, July 1990.
11. G. Antonelli, F. Caccavale, S. Chiaverini, and L. Villani, Tracking control for underwater vehicle manipulator systems with velocity estimation, IEEE J. Oceanic Eng., vol. 25, no. 3, pp. 399-413, July 2000.

12. T. I. Fossen, and M. Blanke, Nonlinear output feedback control of underwater vehicle propellers using feedback from estimated axial flow velocity, *IEEE J. Oceanic Eng.*, vol. 25, no. 2, pp. 241-255, April 2000.
13. J. Yuh, Modeling and control of underwater vehicles, *IEEE Trans. Syst., Man, Cybern.*, vol. 20, pp. 1475- 1483, 1990 D. R. Yoerger, and J. J. E. Slotine, Robust trajectory control of underwater vehicles, *IEEE J. Oceanic Eng.*, vol. OE-10, no. 4, pp. 462-470, 1985.
14. R. Cristi, F. A. Papoulias, and A. J. Healey, Adaptive sliding mode control of autonomous underwater vehicles in the dive plane, *IEEE J. Oceanic Eng.*, vol. 15, no. 3, pp. 152-160, July 1990.
15. A. J. Healey, and D. Lienard, Multivariable sliding mode control for autonomous diving and steering of unmanned underwater vehicles, *IEEE J. Oceanic Eng.*, vol. 18, no. 3. pp. 327-339, 1993.
16. Prester Timothy, Verification of 6 DOF simulation model for REMUS AUV , M.Sc. in ocean and Mechanical Eng. Thesis, MIT, Massachusetts, September-2001